DISCRIMINATION OF FENESTRATE BRYOZOAN GENERA IN MORPHOSPACE

Steven J. Hageman and Frank K. McKinney

ABSTRACT

Concepts for generic diagnoses and discrimination of biserial fenestrate Bryozoa (Fenestellidae) have varied historically, but have largely been based on specialized colony forms (e.g., *Archimedes*), the shape and budding arrangement of chambers and other internal skeletal features such as hemisepta, and occasionally on the presence or absence of discrete characters, such as placement of nodes on the frontal surface (e.g., *Minilya*). The question remains as to whether biserial fenestrate genera represent real biological clades, or whether they are convenient groupings of morphotypes based on untested characters. This study evaluates the distribution of 1075 operational taxonomic units (OTUs) from 15 fenestrate genera with measurements for nine morphometric characters – external features are not emphasized in most generic diagnoses. Here, each OTU represents a composite or idealized individual from a colony. Results show that OTUs plotted in principal component space do largely form coherent clusters based on a priori generic assignments. Thus the groupings based on characters other than the ones used to originally define them, add support to the notion of biological significance for recognized genera. The exceptions actually highlight and help resolve known issues. Therefore, we recognize *Alternifenestella* as a junior synonym of the genus *Spinofenestella*, and propose reassignment of *Laxifenestella serratula* in Snyder (1991) to *Fenestella serratula,* and *Fenestella* sp. 1 in Ernst and Schroeder (2007) as *Rectifenestella*. We do not advocate that biserial fenestrate generic concepts should be based on the nine external characters used in this study, but rather that they can be used independently to evaluate the coherence of genera based on other discrete characters.

Steven J. Hageman. Department of Geology, Appalachian State University, Boone, NC 28608, USA. hagemansj@appstate.edu

Frank K. McKinney. Department of Geology, Appalachian State University, Boone, NC 28608, USA. mckinneyfk@appstate.edu

Editorial note: animations are visible at palaeo-electronica.org/2010_2/206

INTRODUCTION

The purpose of this study is to use characters visible from the exterior of biserial fenestrates to define morphospace occupied by observed taxonomic units (OTUs) assigned to diverse genera and to determine whether OTUs, assigned a priori to a given genus form a distinct cluster within a smaller region of that morphospace. If there is little or no clustering of OTUs assigned to a given genus within the inclusive morphospace, the reality of fenestellid genera based largely on internal characters might be more severely questioned, but distinct clusters of OTUs belonging to those genera supports their discrimination as morphologically characterizable subgroups based on measurable external morphological characteristics (Hageman 1991).

This is a study of genera. The existence of nominal species is acknowledged, but should be considered in the context of within genus variation. The concept of fenestrate species distributions in morphospace will be treated elsewhere.

Historical Summary

In general, the characterization of genera is a subjective enterprise. As more information accumulates, if morphological detail rather than gross morphology is considered more closely, some supposedly well-known genera begin to be reinterpreted as a complex of related but distinguishable genera. The brachiopod genus *Productus* is one of the better known examples, with 29 genera being named in a single volume based on type species originally described as a species of *Productus* (Muir-Wood and Cooper 1960). Fenestrate bryozoans similarly experienced proliferation of generic names during the late 20th century as formerly widely familiar, easily discriminated genera were subdivided.

Fenestrate bryozoans are a major component of the mid- to late Paleozoic marine fossil record. With one known exception, they are characterized by a shared colonial growth habit. They consist of rigidly erect, narrow branches in which all autozooecia open toward one side of the branch (the same direction as neighboring branches), and the number of rows of autozooecial apertures along the branch is limited, varying from two to about ten. Branches typically are laterally linked by anastomosis, by skeletal bars (dissepiments) lacking autozooecia, or by short lateral branches bearing autozooecia . Branch proliferation occurred either by dichotomous division of the growing tip of the branch or by lateral branches (pinnae) that formed on the sides of the parent branch just behind the growing tip. These two types of branch multiplication were used from the late 19th century through most of the 20th century as the basis for the two major taxonomic subdivisions of the fenestrate bryozoan clade (e.g., Bassler 1953), although recently some bryozoan taxonomists have emphasized other morphological characters that result in the mixing of branching types within families (e.g., Morozova 2001). The focus of this study is biserial forms traditionally assigned to the family Fenestellidae.

Early Concepts of Fenestellid Genera. The first genus of fenestrate bryozoans to be characterized in print was *Archimedes*, named by David Dale Owen in 1838 who (p. 13) referred to it only as "...a fossil, described by Lesueur under the name of *Archimedes*, on account of its screw-like form.". The following year, Lonsdale (1839, p. 677) introduced the name *Fenestella* for, "A stony coral, fixed at the base and composed of branches, which unite by growth and form a cup. Externally the branches anastomose or regularly bifurcate; internally they form a network, the intervals being generally oval, one row of pores on the branches externally, the openings being circular and projecting when perfect. The branches, when regularly bifurcated, are connected by distant, transverse processes, in which no projecting pores are visible."

The name *Archimedes* was used in print for solid helical structures a few times between 1838 and 1857, and several species were named from around the world as *Fenestella*. In 1857 Hall (p. 177) recognized that *Archimedes* and *Fenestella* are related and summarized their differences: "In all essential characters, the foliate expansions of *Archimedes* corresponds to *Fenestella*, according to the extended description of this genus by Mr. Lonsdale; and in detached fragments cannot be distinguished generically from other forms of the same genus....The mode of growth, therefore, constitutes the only reliable character for separating *Archimedes* from *Fenestella*; and should this character be hereafter considered of sufficient importance, I propose to retain Le Sueur's original name '*Archimedes*'.

John Phillips (1841) added a third genus, *Hemitrypa*, to the Paleozoic fenestrates soon after *Archimedes* and *Fenestella* were established. Phil-

lips (1841, p. 27) characterized *Hemitrypa* as "...a cup-formed mass; external surface wholly covered with numerous round pores of cells...associated in double rows...The internal face was like that of some *Fenestellæ*, but the peculiarities of the external surface seem to require generic separation." The generic name *Hemitrypa* relates to Phillips' mistaken understanding that the fenestrules extended from the internal surface only halfway through the skeleton. He did not realize that the visible external surface was a superstructure consisting of a finer mesh than the branches, which was developed as an integrated canopy above the branches by proliferation and fusion of lateral processes at the outer ends of long spines extending from the surface of the underlying branches.

The first three genera of fenestrate bryozoans to be characterized were fenestellids in the broad sense, i.e., branches increased by bifurcation rather than developing as pinnae, were laterally linked, and each contained two rows of autozooecia. The differentiation of these three genera foreshadowed characterization of newly named "fenestellid" genera into the late 20th century. That is, "fenestellid" genera were differentiated on the basis of gross colony morphology (*Archimedes* vs. *Fenestella*) or on the basis of meshwork characteristics and/or morphological characteristics visible on branch surfaces (*Fenestella* vs. *Hemitrypa*). There was a roughly parallel development in the characterization of non-pinnate fenestrate bryozoans with three or more rows of autozooecia per branch, but this paper addresses the biserial "fenestellids".

Generic Concepts That Include Internal Characters. Thin sections of fenestrate bryozoans were used extensively by Ulrich (1890) to supplement morphological information available from the surface of colonies, but he did not establish any new fenestrate genera based on thin sections. While not based on prepared thin sections, *Monopora* was named by Lebedev in 1924 based on internal features seen in a corroded specimen. The original illustration of *M. donaica* (Lebedev 1924, Pl. 1, fig. 2) was of a fenestellid fragment that in part showed clearly a single row of triangular to trapezoidal zooecial bases, while in other parts of the drawing what is intended to be portrayed is unclear. According to Nekhoroshev (1932, p. 295), "The third type of [basal fenestellid] section of zooecia appears three cornered. Peculiarities of construction of zooecia of this type as seen in a half destroyed state were mistakenly used by a single author (Lebedev) in the description of a new genus,

Monopora, which is constructed the same as in *Fenestella* but inaccurately described as branches with only a single row of zooecia."

The generic name *Monopora* Lebedev, 1924 has been abandoned. In part, that is because Lebedev's original specimen has apparently been lost, and it is impossible to get a sense of zoarial or zooecial details from his description and illustration. Nikiforova (1933b), in a study of bryozoans from the same region and stratigraphic level, reassigned *Monopora donaica* to *Fenestella* and named three subspecies, *minor*, *media*, and *major*. Termier and Termier (1971) designated *F. donaica* (Lebedev) *minor* Nikiforova as type species of their new genus *Alternifenestella*. Lebedev (1924) gave no scale for the single illustration of *Monopora donaica*, so it is not possible to make any decision about which, if any, of the three subspecies named by Nikiforova (1933b) may include Lebedevs specimen. *F. donaica* (Lebedev) *minor* Nikiforova legitimately stands as type species of *Alternifenestella*.

The next genus initially diagnosed in part on internal structure of the branches was *Minilya* Crockford, 1944. However, between 1924 and 1944 Soviet bryozoan specialists vigorously adopted the use of tangential thin sections to supplement external morphological characterization of fenestrate *species* wherever possible (e.g., Nekhoroshev 1926, 1928, 1932; Nikiforova 1933a-c, 1938). Shul'ga-Nesterenko (1941) recognized five and later (Shul'ga-Nesterenko 1951) 14 morphological groups within the genus *Fenestella* based largely on morphology visible in thin sections, but – although she thought they likely existed – she never named any of the groups as either genera or subgenera.

Proliferation of New Genera. There have been two periods of relatively rapid proliferation of generic names for biserial fenestrates (Figure 1), the 1880s and the late 20th century, especially the 1970s. The increase in the 1880s was due largely to the recognition of several different types of superstructures (Figure 1, 1880s arrow). In contrast the increase in names during the 1970s (Figure 1, 1970s arrow) was due almost entirely to characterization of new genera based on structures visible in thin sections, especially autozooecial morphology and presence of heterozooecia.

The change from biserial fenestrate generic concepts based almost exclusively on external morphology of zoaria and branches to an emphasis on internal morphology seen in thin sections derives in large part from Shul'ga-Nesterenko's work published in 1941 and later. Termier and
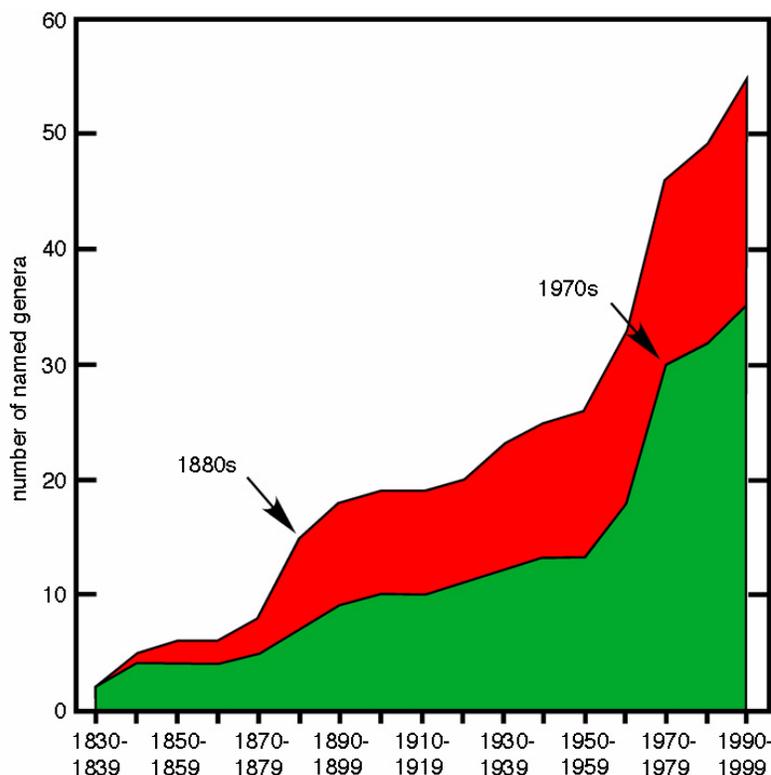
FIGURE 1. Cumulative number of named biserial, non-pinnate fenestrate genera by decade from the first genus named in 1838. The arrows indicate decades of relatively rapid proliferation of generic names; several genera characterized by superstructures (red) were named during the 1880s, and during the 1970s several genera that lack superstructures (green) were named. The curves reflect all validly published generic names, whether or not they are widely accepted as well founded, or are generally considered to be junior synonyms.

Termier (1971) used Shul'ga-Nesterenko's informal groups based on details visible in thin sections to split off five new genera from *Fenestella,* although two of the five are invalid because no type species was designated from among the several species included in the intended new genus. This paper stimulated Morozova to revise the generic concept of *Fenestella* and to formalize several more of Shul'ga-Nesterenko's informal groups, and she named 10 new fenestellid genera (Morozova 1974). Since the 1970s almost all newly proposed genera of biserial fenestrates have been based largely or entirely on internal morphology visible in thin sections.

Characters Used in Generic Diagnoses. Features that are most clearly seen or are visible only in thin sections of species of *Fenestella sensu latu* include characters such as: 1) presence or absence of heterozooecia, 2) alignment of median obverse nodes in a linear or a zigzag row; and features of the autozooecia such as 3) presence or absence of hemisepta and (rarely) complete diaphragms, 4) angles of intersection of the transverse wall with the reverse and axial walls, 5) degree of internal overlap of the two rows of autozooecia along the branch and whether that degree of overlap is relatively constant from obverse to reverse side or increases toward the reverse side, 6) overall chamber size, and 7) the ratio of chamber length:width:height. Except presence or absence of heterozooecia and of hemisepta and diaphragms within autozooecia, these characters are continuous rather than discrete. Most characters visible on the skeletal surface are also continuous, such as 1) degree of branch sinuosity, 2) distance between dissepiments, 3) shape of fenestrules, 4) robustness of branches and 5) dissepiments, 6) presence of an axial keel, 7) spacing and 8) diameter of any nodes on the keel, 9) size and 10) position of autozooecial apertures and 11) their proximity to the median plane (i.e., keel, if present).

The vigorous subdivision of *Fenestella s.l.* into new genera, begun in the early 1970s, was not received well by V.P. Nekhoroshev, who along with

his wife (A.I. Nikiforova) during the 1920s through 1940s had established inclusion of thin section observation as a matter of course for understanding characteristics of fenestrate species. He laid out his objections (Nekhoroshev 1979) in unambiguous terms in a paper titled "O neratsionalnosti razdeleniya roda *Fenestella*" ("On the non-rational subdivision of the genus *Fenestella*"). He considered the newly named genera to be junior synonyms of *Fenestella* and to be based on arbitrary and subjective boundaries within a single genus.

Indeed the majority of taxonomic characters within *Fenestella s.l.* are continuous, which means that some decisions about assignment of species to a genus split off from *Fenestella s.l.* are difficult to make. Characters and character combinations that make for difficult assignments include angle of intersection of the transverse interzooecial wall with the axial wall that divides the two rows of zooecia and with the reverse wall, as well as the degree of overlap of the chambers of the two rows of autozooecia along a branch. The overlap of autozooecial rows ranges from nonexistent (linear axial walls) to complete overlap basally, which results in triangular cross sections of chambers and no distinction between transverse and axial walls between autozooecia. In some cases (e.g., Ernst and Winkler Prins 2008) a high proportion of fenestellid species in a study end up being questionably assigned to one or another of the fenestellid genera.

MATERIALS AND METHODS

Species of biserial fenestrates that are characterized by dichotomous branching and branch linkage by dissepiments, either described in literature published from 1980 to 2007 or identified and characterized in unpublished post-1980 data sets available to us, were considered for this study. Species accepted for inclusion in the study (Appendix) had to meet certain criteria: 1) Assignment to genus by the author of the paper or data set based on the contemporary criteria of zooecial characteristics visible in thin sections plus geometry of the keel node sequence (i.e., whether in uniserial or biserial rows), plus 2) a minimum set of measurements made from the exterior surface in addition to information from thin sections used by the author for discrimination of fenestellid genera.

Data for this study were compiled from nine sources using the criteria given above (McKinney and Kriz 1986; Snyder 1991; Holdener 1994; McColloch et al. 1994; Nakrem 1994; Nakrem 1995; Ernst 2001; Ernst and Schroeder 2007; and

McKinney, unpublished data). Each of the 15 genera used in this study is represented by 12 to 273 composite OTUs from 1 to 9 species per genus (Appendix).

Two species included in the study, *Lyroporella serissima* (Nakrem 1995) and *Anastomopora anaphora* (McColloch et al. 1994) are not biserial fenestellids but were intended to serve as reference points. Their branch organization differs from fenestellids in having three or more rows of zooecia except proximal to branch bifurcations. If the position of the two genera in morphospace were isolated from a tightly clustered cloud comprised of all the fenestellid species included herein, then any differences in position of the multispecies fenestellid genera within the cloud would indicate relatively trivial differences in gross morphology. If, however, the two extraneous species of *Lyroporella* and *Anastomopora* were within or contiguous with the fenestellid cloud, then any notable differences in distribution of multispecies fenestellid genera within the cloud could be interpreted to represent appreciable differences in gross morphology among genera.

Lyroporella serissima (Nakrem, 1995) has branches organized like those of *Polyporella*, with two rows of zooecia distal to bifurcations but proliferating to three rows at an appreciable distance preceding the next bifurcation. Nakrem (1995) followed the understanding of McKinney (1994) that such lyre-shaped fenestrates are species of the genus *Lyropora*. McKinney (1994) had missed that Miller (1889) listed *Fenestella* (*Lyropora*) *lyra* Hall, 1857 as type species of *Lyropora* and thought that Ulrich's 1890 designation of *F.* (*Lyropora*) *quincucialis* Hall, 1857 as type species of *Lyropora* was the earliest. Thinking that *F.* (*Lyropora*) *quincucialis* Hall had been the earliest designated type species of *Lyropora*, Simpson's designation (Simpson 1897) of the same species as type species of *Lyroporella* Simpson, 1895 was considered to make *Lyroporella* a junior objective synonym of *Lyropora*. *Lyroporella* is a different genus from *Lyropora* based on the type species *F. (Lyropora) lyra*, which has polyserial zooecial rows in branches, requiring reassignment of Nakrem's (1995) species *Lyropora serrisima* to *Lyroporella*. The second is a species of *Anastomopora*, which typically has multiserial branches. However in some species − such as *Anastomopora anaphora* (McColloch et al. 1994) included here − branch segments begin with only two rows of zooecia after a bifurcation before interpolating additional rows of zooecia. McColloch et al. (1994) named the spe-
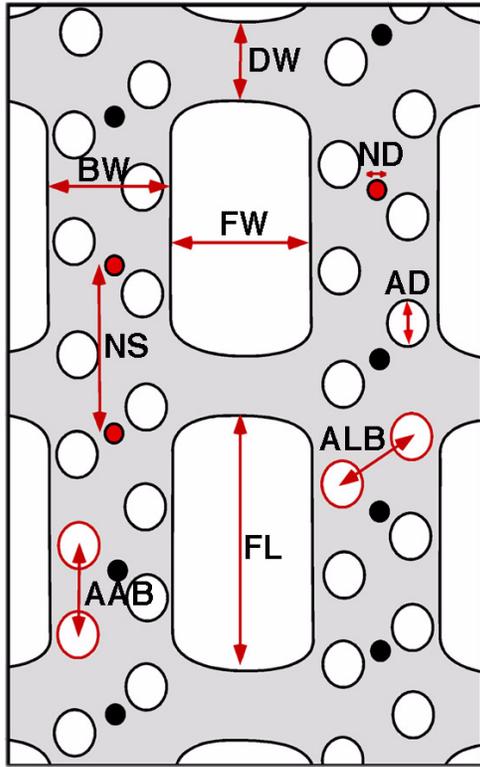
FIGURE 2. Idealized fenestrate bryozoan illustrating the position of the nine measured characters and their end-member descriptors: Branch Width **(**BW, narrow vs. wide), Dissepiment Width (DW, narrow vs. wide), Fenestrule Length **(**FL, short vs. long), Fenestrule Width **(**FW, narrow vs. wide), Aperture Diameter **(**AD, small vs. large), Aperture spacing Laterally across Branch (ALB, close vs. distant), Aperture spacing Along Branch (AAB, close vs. distant), Node Diameter (ND, small vs. large), Node Spacing **(**NS, close vs. distant).

cies *Reteporidra anaphora*. We have reassigned it to *Anastomopora* Simpson, 1897, because we consider *Reteporidra* Nickles and Bassler (1900) (nom. nov. pro *Reteporella* Simpson 1895, *non* Busk 1884) to be a junior subjective synonym of *Anastomopora* Simpson 1897.

Morphological Characters

Nine morphological characters that could be measured from the exterior surface were selected for our data set: Branch Width (BW), Fenestrule Length (FL), Fenestrule Width (FW), Dissepiment Width (DW), Aperture Diameter (AD), Aperture spacing Laterally across Branch (ALB), Aperture spacing Along Branch (AAB), Node Diameter (ND), Node Spacing (NS), as indicated in Figure 2. These characters were selected because: 1) they were present (available) on a majority of species

available for consideration, and 2) data for equivalent characters had been collected by a majority of recent authors. The criteria for inclusion were pragmatic, based on availability of data rather than a priori biological significance. However, these characters have appropriate qualities for this study because: 1) they are *not* typically used in generic-level diagnoses and descriptions; 2) these characters have demonstrated significance at some level of taxonomic discrimination (e.g., Snyder and Gilmour 2006; Ernst et al. 2008); and 3) these characters will continue to be used by future workers based on their availability.

It is beyond the scope of this paper to infer evolutionary significance of the differentiation of character states among fenestrate bryozoan genera; however, the relationship between skeletal morphology and biologically and ecologically significant soft-part characters has been described (e.g., Winston 1977, 1978; McKinney and Jackson 1991).

Types of Data

The fundamental datum in this study is a "composite OTU." Each data point in the following figures of PCA scatter plots consists of a vector of the nine measured characters collected from the same colony. This datum represents an idealized OTU at the level of an individual module in the colony, but limitations do not allow for measurement of all nine characters from a single zooecium (e.g., meshwork vs. zooecial characters). Correlation of characters within a single composite may or may not have real significance. Composite OTUs in this study are represented by two kinds of data.

Raw Measurements in Millimeters. For specimens where original measurements were available, most measurements were measured from multiple colony fragments, identified by the original author as conspecific (Appendix, Data Type = measured). Typically 12 to 24 measurements were available per species. In some cases many (100 to 200) measurements per species were available. In other cases very few (2 to 4) composite OTUs could be constructed from available raw measurements.

Scores Reconstructed from Summary Statistics. For specimens where original measurements were not available, 12 composite OTUs were reconstructed using published summary statistics (mean, standard deviation, minimum and maximum values) using Normal Order Deviates (see Hageman et al. 2009). The goal of this exercise was to *approximate* the multivariate hyper-volume

TABLE 1. Parameters used to reconstruct composite OTUs from summary statistics. Example from Nakrem (1995), *Alternifenestella* cf. *tenuiseptata*. Definition for character abbreviations in Figure 2, "original" in black are summary statistics from Nakrem (1995), "reconstructed" in blue are summary statistics calculated from normal order deviates (Table 2) – SD = standard deviation, Min = minimum value, Max = maximum value, n = number of measurements/reconstructed data scores. Character abbreviations are given in Figure 2.

Summary Statistics for *Alternifenestella* cf. *tenuiseptata*.

Data	Type	Mean	SD	Min	Max	n
BW	original	0.234	0.030	0.180	0.290	29
	reconstructed	**0.234**	**0.028**	**0.185**	**0.283**	**12**
DW	original	0.129	0.035	0.080	0.180	30
	reconstructed	**0.129**	**0.0331**	**0.072**	**0.186**	**12**
FL	original	0.592	0.082	0.490	0.760	31
	reconstructed	**0.592**	**0.0776**	**0.458**	**0.726**	**12**
FW	original	0.362	0.036	0.290	0.440	31
	reconstructed	**0.362**	**0.0341**	**0.303**	**0.421**	**12**
AD	original	0.094	0.009	0.080	0.110	9
	reconstructed	**0.094**	**0.0085**	**0.079**	**0.109**	**12**
ALB	original	0.252	0.018	0.210	0.280	25
	reconstructed	**0.252**	**0.0170**	**0.223**	**0.281**	**12**
AAB	original	0.200	0.013	0.170	0.220	22
	reconstructed	**0.200**	**0.0123**	**0.179**	**0.221**	**12**
ND	original	0.082	0.031	0.050	0.110	4
	reconstructed	**0.083**	**0.0270**	**0.045**	**0.110**	**12**
NS	original	0.301	0.025	0.250	0.330	10
	reconstructed	**0.301**	**0.0237**	**0.260**	**0.342**	**12**

represented by 12 composite OTUs (Appendix, Data Type = reconstructed). No assumptions were made about reconstructed scores representing the distribution and covariate structure of original data, only that their overall position in multivariate space would approximate that of normally distributed samples with an equivalent mean and variance. Table 1 provides an example of the calculation. The steps include:

1. Obtain summary statistics for measured values associated with a published description, preferably with five or more observations per character, reflecting measurements compiled from three or more specimens (Table 1).

2. Identify the Normal Order Deviates for n= number of observations (here 12) from a sample with a normal distribution, mean of zero and standard deviation of one (Rohlf and Sokal 1981, table 37; Hageman 1992) see Table 2, column NOD.

3. Reconstruct 12 scores for each character using the equation:
   mean + (standard deviation x normal order deviate)
   This results in 12 scores that have the approximate distribution (mean and sample deviation) as the original measured sample (Table 2).

4. For each character and each putative species, compare values of observed vs. reconstructed mean, standard deviation, minimum, and maximum (Table 1). In some cases, some reconstructed values were modified by hand in order to better approximate the observed distribution and summary values (Table 2, highlighted red).

5. Within each column (character), reconstructed scores were randomized independently by column. Rows resulting from the independent randomization by columns provide 12 com-

TABLE 2. Scores reconstructed from data in Table 1 using the formula: GS = M + (SD x NOD), where M = mean value for a measured character from a putative species, SD = standard deviation for the same sample, and NOD is the normal order deviate expected from a sample of n = 12, with a mean of zero and standard deviation of one (Rohlf and Sokal 1981, table 37). Definition for character abbreviations are given in Figure 2. Values in red (ND) were altered in order for the values of mean, SD, Min, and Max from reconstructed scores to more closely approximate observed summary statistics. Min and max are a comparison of the respective reconstructed score with the observed values, expressed a percentage difference from the original. Twelve composite OTUs were reconstructed by randomizing the position of each value, independently by column (character).

Scores for *Alternifenestella* cf. *tenuiseptata* reconstructed using summary statistics and normal order deviates

NOD	BW	DW	FL	FW	AD	ALB	AAB	ND	NS
-1.62923	0.185	0.072	0.458	0.303	0.079	0.223	0.179	0.045	0.260
-1.11573	0.201	0.090	0.501	0.322	0.084	0.232	0.185	0.047	0.273
-0.79284	0.210	0.101	0.527	0.333	0.087	0.238	0.190	0.052	0.281
-0.53684	0.218	0.110	0.548	0.343	0.089	0.242	0.193	0.065	0.288
-0.31225	0.225	0.118	0.566	0.351	0.091	0.246	0.196	0.072	0.293
-0.10259	0.231	0.125	0.584	0.358	0.093	0.250	0.199	0.079	0.298
0.10259	0.237	0.133	0.600	0.366	0.095	0.254	0.201	0.085	0.304
0.31225	0.243	0.140	0.618	0.373	0.097	0.258	0.204	0.110	0.309
0.53684	0.250	0.148	0.636	0.381	0.099	0.262	0.207	0.099	0.314
0.79284	0.258	0.157	0.657	0.391	0.101	0.266	0.210	0.115	0.321
1.11573	0.267	0.168	0.683	0.402	0.104	0.272	0.215	0.117	0.329
1.62923	0.283	0.186	0.726	0.421	0.109	0.281	0.221	0.110	0.342
min	2.19%	-6.22%	-5.34%	3.69%	-0.71%	5.03%	4.41%	-6.10%	3.41%
max	-3.04%	4.67%	-5.81%	-5.34%	-1.42%	0.53%	0.59%	0.00%	3.90%

posite OTUs. As a result, there is no natural correlation among characters within a reconstructed OTU, but this process removes the primary linear relationship and helps to maximize the hyper-volume occupied by the samples in multidimensional morphospace.

Combination of Raw and Reconstructed Data. In a few cases, where full suites of measured data were available for most specimens, but only a partial suite was available for one or two characters (e.g., unmeasurable from available material), the full suite of composite OTUs was created by reconstructing scores for the missing data using methods above. These taxa include: *Apertostella crassata, Hemitrypa bohemicus, Hemitrypa mimicra, Hemitrypa tenella,* and *Laxifenestella digittata*.

Transformation of Data

The completed data set (1075 composite OTUs x 9 Characters) was transformed by standardizing the data (Z-score), where the mean and standard deviation were calculated across *all* OTUs for each character. The values for transformed OTUs are expressed in units of standard deviation from a mean of zero. This removes differences among characters measured at different scales, so that analyses will emphasize relative variation and not emphasize absolute scale.

Principal Components Analysis

Principal Components Analysis was performed with the software PAST v. 1.81 (Hammer et al. 2001). Eigen values, the cumulative percentage of variance explained by each, the loading coefficients for each axis and PCA scores for each composite OTU on all nine axes were saved for evaluation.

Contribution of Individual Characters to Principal Component Axes. The relative correlation (importance) of each of the nine morphometric characters to each of the PCA axes was evaluated by examining the loading coefficients. Important

characters for PCA axes 1 to 5 (largest absolute values) were highlighted by annotating representative scatter plots with idealized illustrations of specimens with end-member states for the character.

A variance-covariance matrix was also calculated using PAST v. 1.81 (Hammer et al. 2001) in order to evaluate relationships among characters.

Generating Three-Dimensional (3-D) Scatter Plots and Animations. A variety of three- dimensional graphs were created using the "Scatterplot 3-D" function in JMP (PCA scores exported from PAST via text file), with the goal to: 1) characterize overall variation within and among all genera, 2) illustrate variation accounted for by different principal component axes, and 3) highlight differences among closely related genera (plotted in a morphospace defined by all genera).

Animated files of three-dimensional scatter plots were generated using the following procedure: 1) graphs were rotated to a standard starting orientation with the intersect of negative axes in the lower center of screen, 2) the plot was saved as a jpeg file, 3) plot was rotated 6°, 4) steps 2 and 3 were repeated through 360°, generating 60 jpeg files, 5) all files were scaled 60% using the batch image converter application Resizeit v. 2.3.1 (SYWSoft), and 6) an animated gif file was created using the application GIFfun v. 4.2 (Stone Design Corp.), with a 0.13 second delay between frames.

Data Subsets in Scatter Plots and 3-D Animations. The large amount of data employed in this study makes visual interpretation of the entire 1075 OTU data set difficult. Nevertheless, the following plots were generated: 1) All genera, PCA 1 vs. 2 vs. 3, 2) All genera, PCA 3 vs. 4 vs. 5 and 3) All genera, PCA 6 vs. 7 vs. 8. In order to see relationships among genera more clearly, subsets of the data (all calculated in the same multivariate space) were plotted individually. The genus *Rectifenestella* was used as a standard for comparison in many of these plots.

RESULTS

Each symbol (grey circle or colored sphere) on scatter plots in figures of this paper represents a composite OTU, which is the set of measurements for nine morphological characters from a single fenestellid colony. When viewing and interpreting the PCA scatter plots, the reader should keep in mind that: 1) each symbol represents an "observation" from a colony = nine measurements; 2) each color represents a bryozoan systematist's generic identification for the specimen from which the data

TABLE 3. Eigenvalues for each Principal Component axis, the variance explained by each axis, and the cumulative amount of variance explained by multiple axes (e.g., first four axes account for 74.8% of total variance).

PCA Axis	Eigen-value	Percent Variance	Cumulative % Variance
1	3.66	40.6	40.6
2	1.16	12.9	53.5
3	1.02	11.3	64.9
4	0.89	9.9	74.8
5	0.67	7.5	82.2
6	0.52	5.8	88.0
7	0.48	5.4	93.4
8	0.32	3.6	97.0
9	0.27	3.0	100.0

were collected; 3) each group of symbols representing a genus consists of a variable number of species, colonies and composite observations per colony; and 4) for the most part, the original and traditional generic diagnoses for these taxa did *not* include any of the nine characters used in these plots (i.e., these plots represent relationships among characteristics typically not used to define the taxonomic concept of any of the genera).

The first results section characterizes each Principal Component Axis, i.e., which characteristics are most important for the axis and which regions of the plots will reflect which characters. This section also describes whether the axes differentiate variation *among* genera (have taxonomic value) or variation *within* genera (variation among and within species and individuals). Details are reserved for the second results section, which summarizes the distribution of genera within the defined morphospace.

Principal Component Axes

Among Genera vs. Within Genera Variation. The distribution of specimens expressed on Principal Component Axes one through five (PCA-1 to PCA-5) primarily reflect variation *among* genera and collectively account for 82.2% of the observed variation (Table 3).

The relationship between the positions of data points (colony-level observations) and the character states for morphological features with which the axes are most correlated is represented in Figure 3 for PCA-1 and PCA-3. These same data, plotted on PCA-1, PCA-2, and PCA-3, are color coded to represent generic assignment in Figure 4, which is
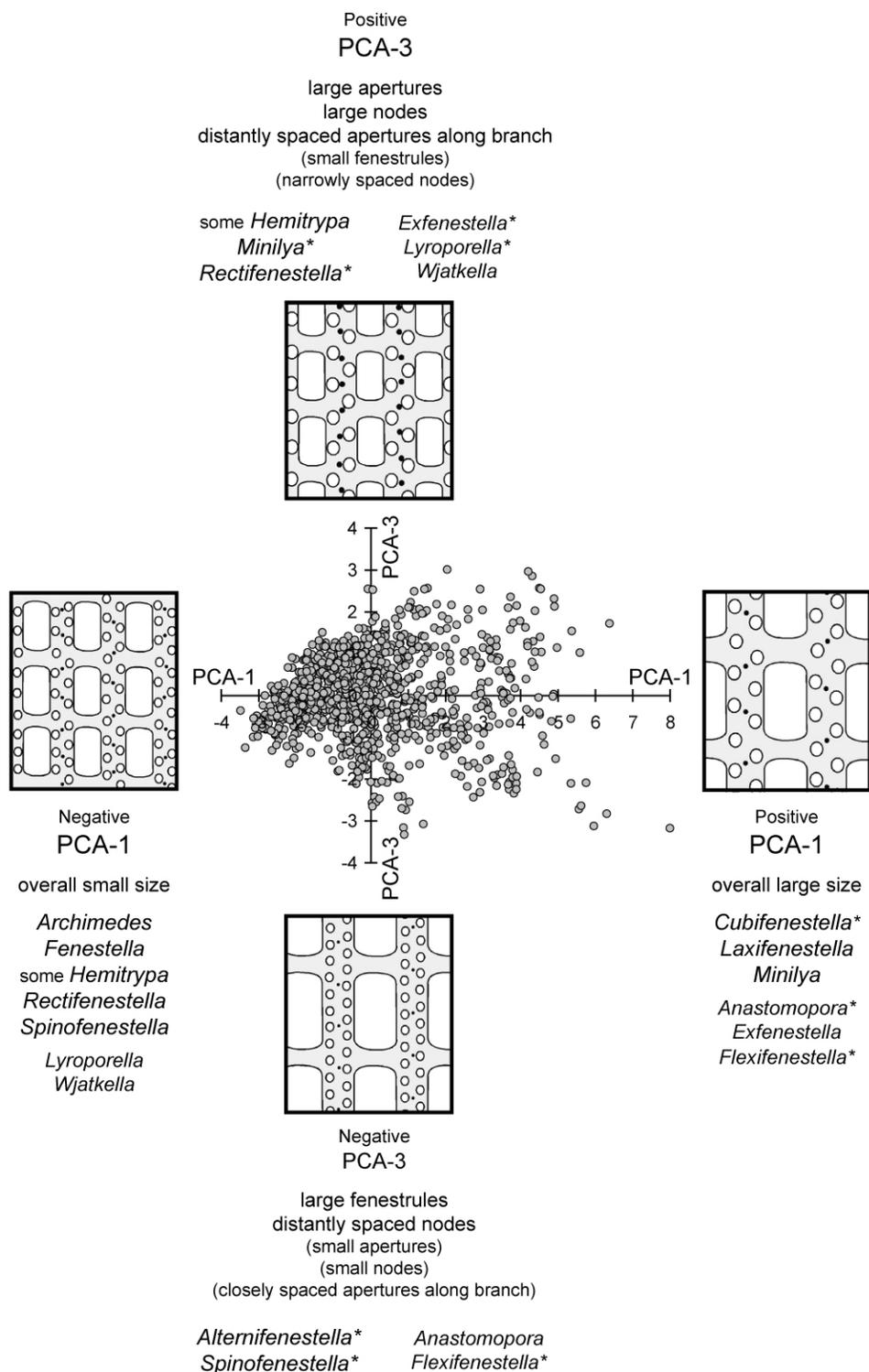
FIGURE 3. Scatter plot of PCA-1 vs. PCA-3, which combined account for 51.9% of the total variance. PCA-1 is positively correlated with the size of each of the nine characters in approximately equal weight (Table 4). PCA-3 reflects an inverse relationship between the size of apertures and nodes and spacing of apertures vs. the size of fenestrules and spacing of nodes (Table 5). Figure 4 is an inclined, three-dimensional view of this image. The only two genera that do not display a cohesive cloud with a predictable distribution on PCA-1 are *Alternifenestella* and *Apertostella*. Five genera (*Apertostella*, *Archimedes*, *Cubifenestella*, *Fenestella,* and *Laxifenestella* are centered (no predictable distribution) on PCA-3.
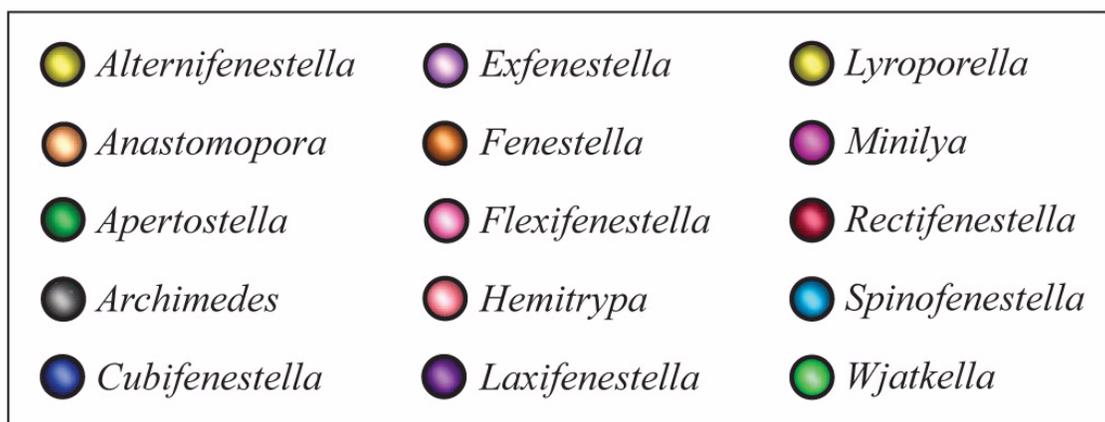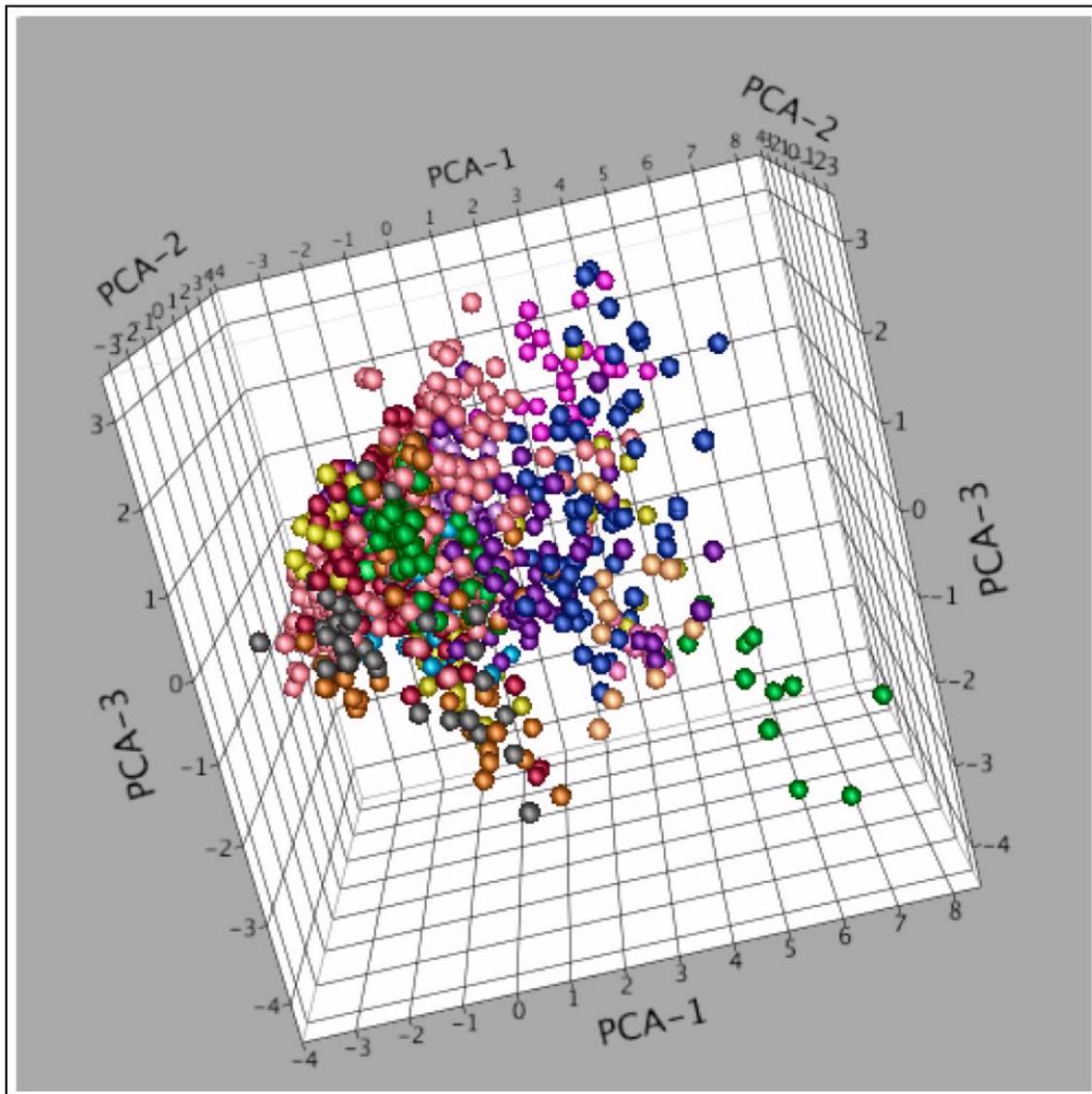
FIGURE 4. Scatter plot of all genera for PCA-1 vs. PCA-2 vs. PCA-3, which combined account for 64.9% of the variance. This view permits an evaluation of distributions along PCA-1 and PCA-3. Animation of the three axes in rotation is provided by Animation 1, which can also be accessed via the Animation Menu. Figure 3 is an orthogonal view (PCA-1 vs. PCA-3) of this image.

linked to an animation of the axes in rotation (Animation 1). All animations in this paper can be accessed either directly by hyperlinks from the text, or via the Animation Menu. The relationship between the positions of data points and the character states for morphological features with which the axes are most correlated for PCA-2 and PCA-3 is represented in Figure 5. These same data, plotted on PCA-1, PCA-2, and PCA-3, are color coded to represent generic assignment in Figure 6, which is linked to an animation of the axes in rotation (Animation 1). The relationship between the positions of data points and the character states for morphological features with which the axes are most correlated for PCA-4 and PCA-5 is represented in Figure 7. These same data, plotted on PCA-3, PCA-4, and PCA-5, are color coded to represent generic assignment in Figure 8, which is linked to an animation of the axes in rotation (Animation 2).

Principal Component Axes six through nine (PCA-6 to PCA-9) primarily reflect variation within genera and collectively account for 17.8% of the observed variation (Table 3). Data points (colony-level observations color coded to represent generic assignment) are plotted on PCA-6 and PCA-7, and on PCA-8 and PCA-9 in Figure 9. These same data are plotted on PCA-6, PCA-7, and PCA-8 in Figure 10, which is also linked to an animation of the axes in rotation (Animation 3).

PCA-1: Size. Principal Component Axis One represents overall size for all characters (Table 4, column 1) and provides differentiation among most genera (Table 5, Figure 3). All characters are about equally weighted, with emphasis on fenestrule size (FL and FW), slightly less weight on Aperture spacing Laterally across Branch (ALB) and node spacing and size (NS, ND), and the least on other characters.

In Figures 3 and 4, specimens with large values for all characters plot high on PCA-1 (positive = right on Figure 3) and those with the collectively smallest values for all characters plot low (negative = left) on PCA-1. There is a finite size limit on the negative part of PCA-1 (absolute smallest size in reality and observed). As a result, there is more room to expand in size and specialize in the positive direction of PCA-1 (minimum value is -3.5, whereas the maximum value is 8.0) (Figures 3 and 4). Values are negatively skewed on PCA-1 with a median of -0.289. The size trend is evident when the data cloud is viewed in three dimensions PCA-1 vs. PCA-2, vs. PCA-3 (Figure 4). By definition (all characters having approximately equal weight on

PCA-1) large values are excluded from each of the remaining axes when scores are low on PCA-1. This autocorrelation results in a conical shape of the overall cloud (narrowing to the left on Figures 3 and 4 and when PCA-1 is included in any scatter plot.

PCA-2: Aperture Size vs. Spacing, Plus Dissepiment Width. PCA axis two represents an inverse relationship between the size of an aperture (AD) vs. aperture spacing along the branch (AAB) and provides differentiation among several genera (Table 5, Figure 5). Thus, small apertures have greater spacing between them (Table 5). Specimens with large values for Aperture Diameter (AD) plot low on PCA-2 (to the left on Figure 5) and those with large aperture spacing along branch (AAB) plot high on PCA-2 (to the right on Figure 5). Axis two also displays a positive relationship between the size of apertures (AD) and Dissepiment Width (DW), e.g., wide dissepiments are associated with more closely spaced apertures along branch (Table 5). Several genera are differentiated on PCA-2, especially those that plot relatively high on PCA-1. Otherwise, the specimen cloud is centered near zero on PCA-2 (Figure 5).

PCA-3: Fenestrule Size vs. Aperture Size and Spacing. Axis three represents an inverse relationship between the size (openness) of fenestrules and the size and spacing of apertures and provides differentiation among several genera (Table 5, Figure 5). Specimens with larger, more open fenestrules and small, closely spaced apertures plot low on PCA-3 (to the bottom of Figure 5), whereas those with smaller fenestrules and larger, more distantly spaced apertures plot high (to the top on Figure 5). Principal Component axis three also reflects an inverse relationship between node spacing vs. size (NS vs. ND). Specimens with larger diameter nodes plot higher on PCA-3 (to the top on Figure 5), whereas those with a greater spacing between nodes plot lower on PCA-3 (to the bottom on Figure 5). The distribution of samples on PCA-3 can also be evaluated on Figures 6.

PCA-4: Branch and Dissepiment Width vs. Node Size and Spacing and Aperture Size. Axis four represents an inverse relationship between the combined size (width) of branches and dissepiments (= robustness) relative to the size and spacing of nodes and aperture size (diameter) (Table 4). PCA-4 provides some differentiation among several genera (Table 5, Figure 7). Specimens with wider branches and dissepiments and smaller more closely spaced nodes plot low (to the left on
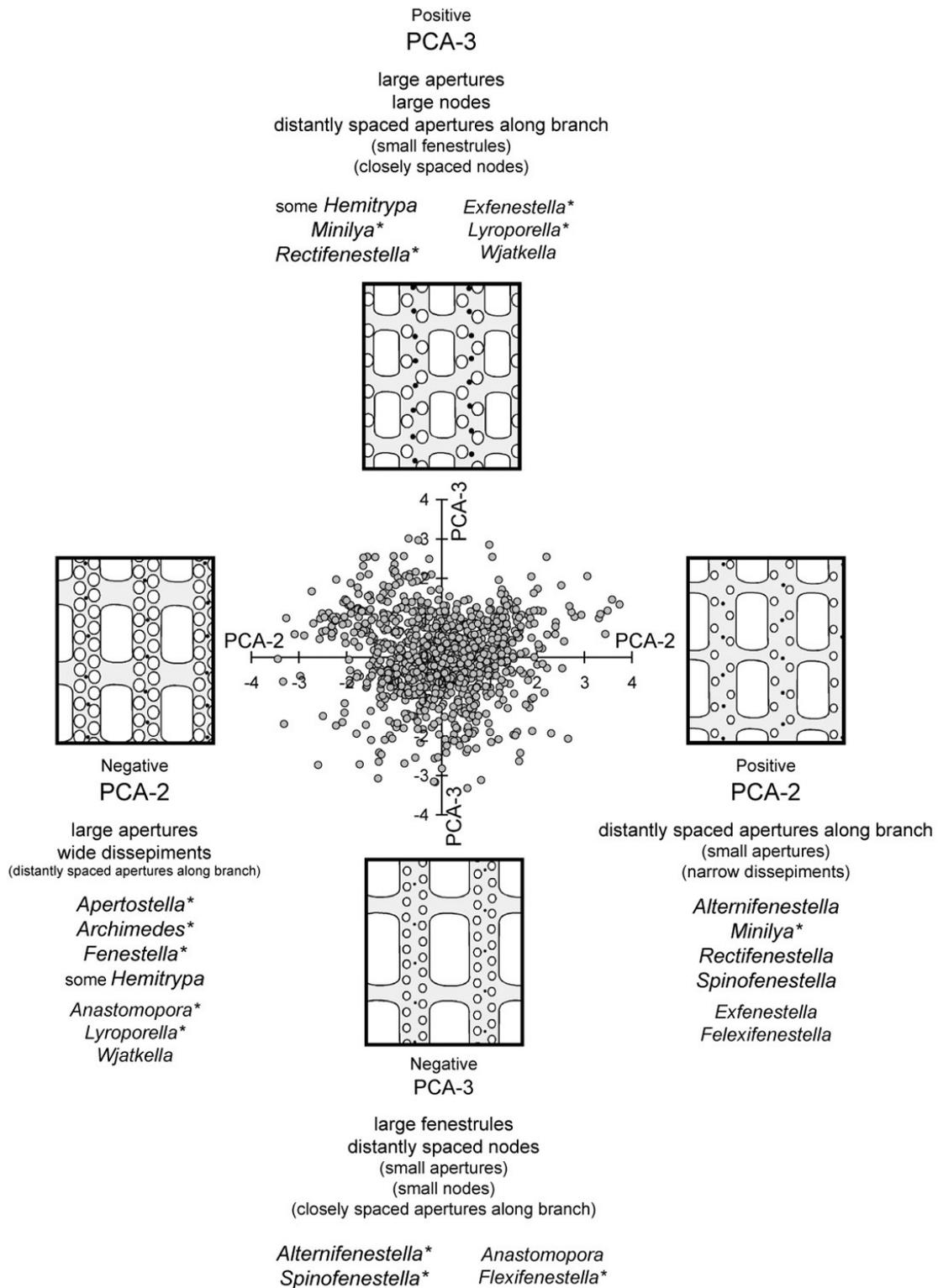
FIGURE 5. Scatter plot of PCA-2 vs. PCA-3, which combined account for 24.2% of the total variance. PCA-2 reflects an inverse relationship between size of apertures and their spacing along branch (Table 4). PCA-3 reflects an inverse relationship between the size of apertures and nodes and spacing of apertures vs. the size of fenestrules and spacing of nodes (Table 5). Figure 6 is an inclined, three dimensional view of this image. Three genera, *Cubifenestella*, *Hemitrypa*, and *Laxifenestella* are centered (no predictable distribution) on PCA-2.
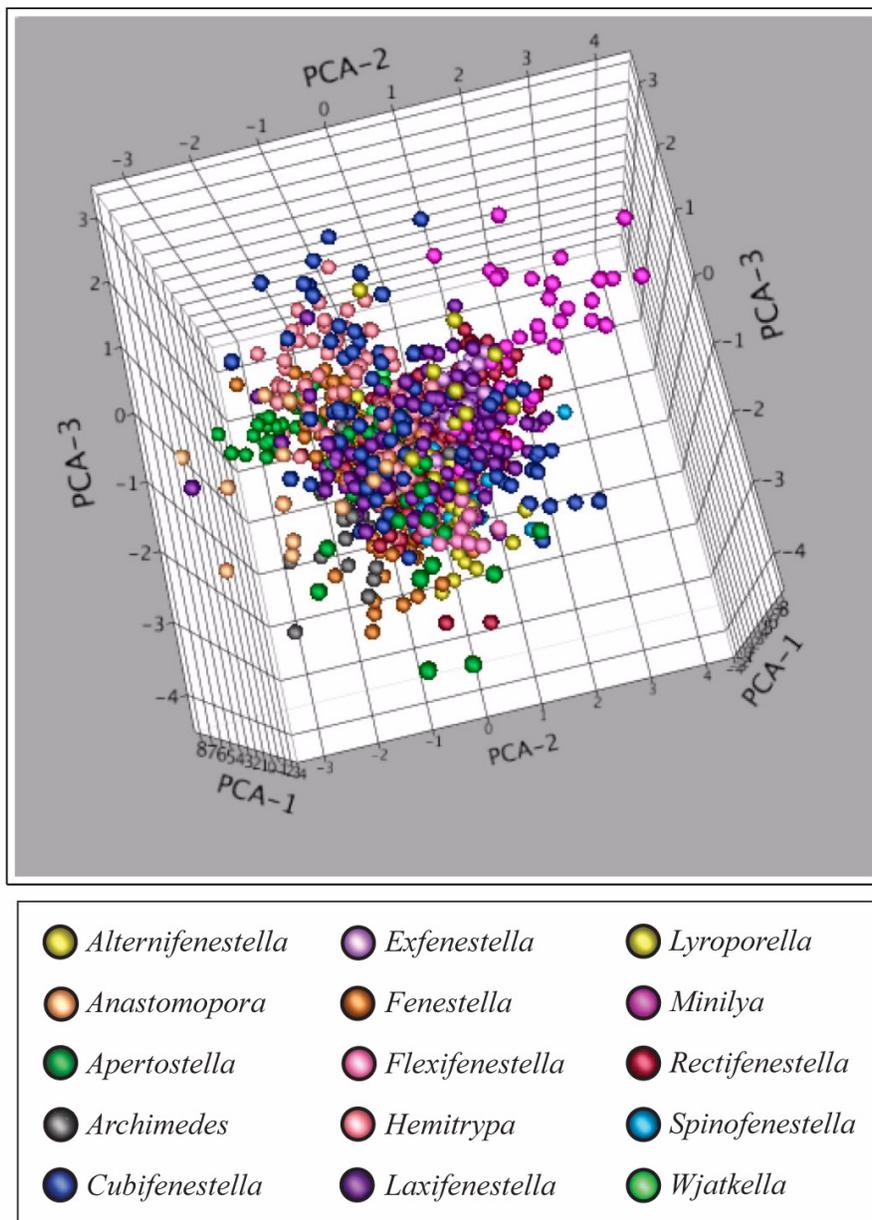
FIGURE 6. Scatter plot of all genera for PCA-1 vs. PCA-2 vs. PCA-3, which combined account for 64.9% of the variance. This view permits an evaluation of distributions along PCA-2 and PCA-3. Animation of the three axes in rotation is provided by Animation 1, which can also be accessed via the Animation Menu. Figure 5 is an orthogonal view (PCA-2 vs. PCA-3) of this image.

Figure 7), whereas those with more narrow branches and dissepiments and larger more distantly spaced nodes plot high (to the right on Figure 7). The distribution of samples on PCA-4 can also be evaluated on Figure 8.

Most taxa cluster near the center of PCA-4 (zero on Figure 7), but some generic groups do differentiate along PCA-4, so therefore combined characters BW, DW, ND, NS and AD have significance for differentiating among some fenestellid genera.

PCA-5: Dissepiment Width, Aperture Spacing, and Node Diameter vs. Aperture Size and Spacing. Axis five does not represent a simple relationship among characters with obvious biological links (Table 5). Specimens with larger apertures (AD)
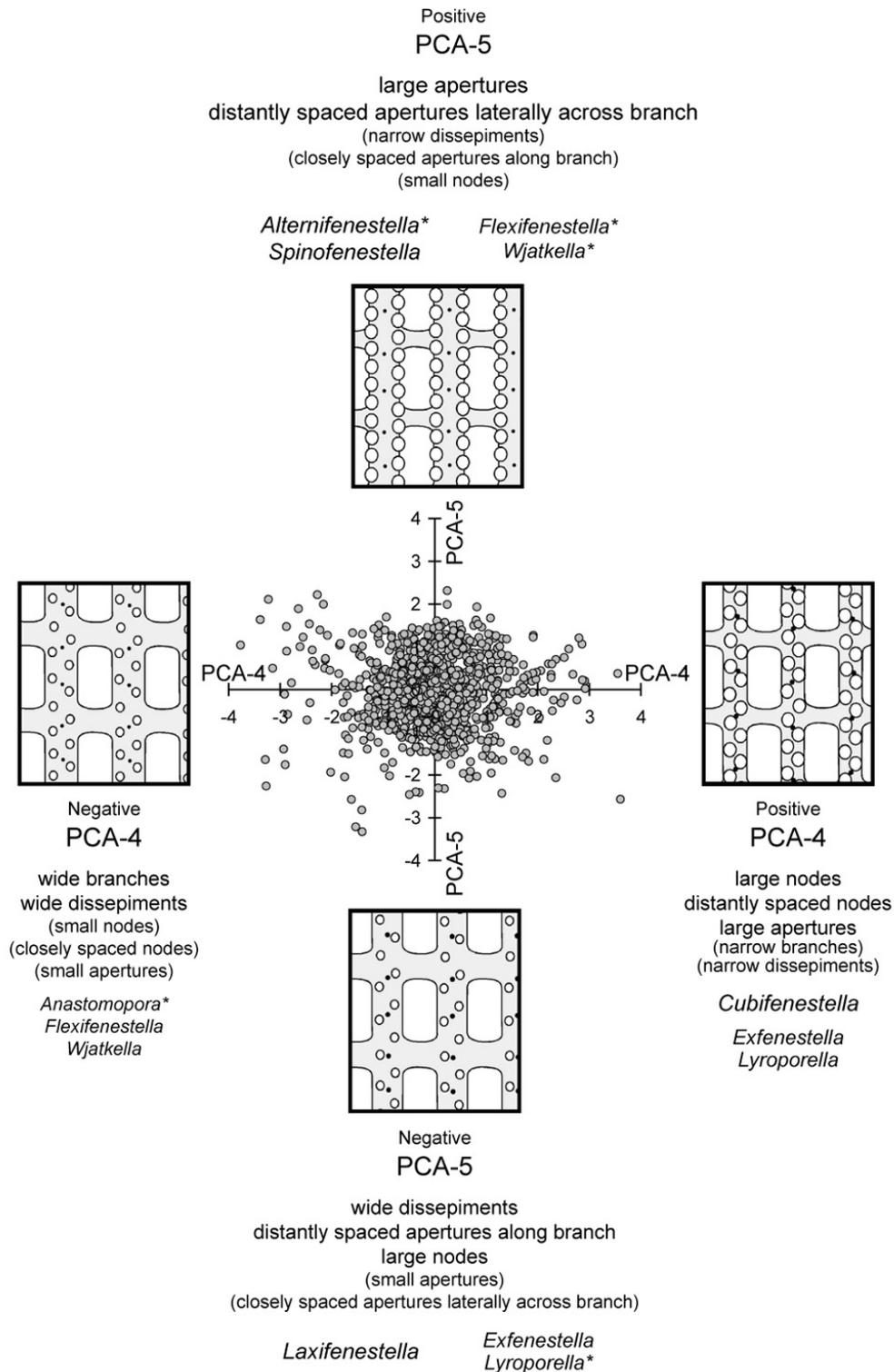
FIGURE 7. Scatter plot of PCA-4 vs. PCA-5, which combined account for 17.4% of the total variance. PCA-4 reflects an inverse relationship between the size and spacing of nodes with aperture size vs. the width of branches and dissepiments (Table 4). PCA-5 reflects an inverse relationship between the size of apertures and their lateral spacing across branches vs. the width of dissepiments, spacing of apertures along branch and size of nodes (Table 5). Figure 8 is an inclined, three-dimensional view of this image. Only one genus, *Cubifenestella*, has a notable distribution on PCA-4, whereas three genera, *Alternifenestella*, *Spinofenestella,* and *Laxifenestella* have notable distributions defined by characters associated with PCA-5.
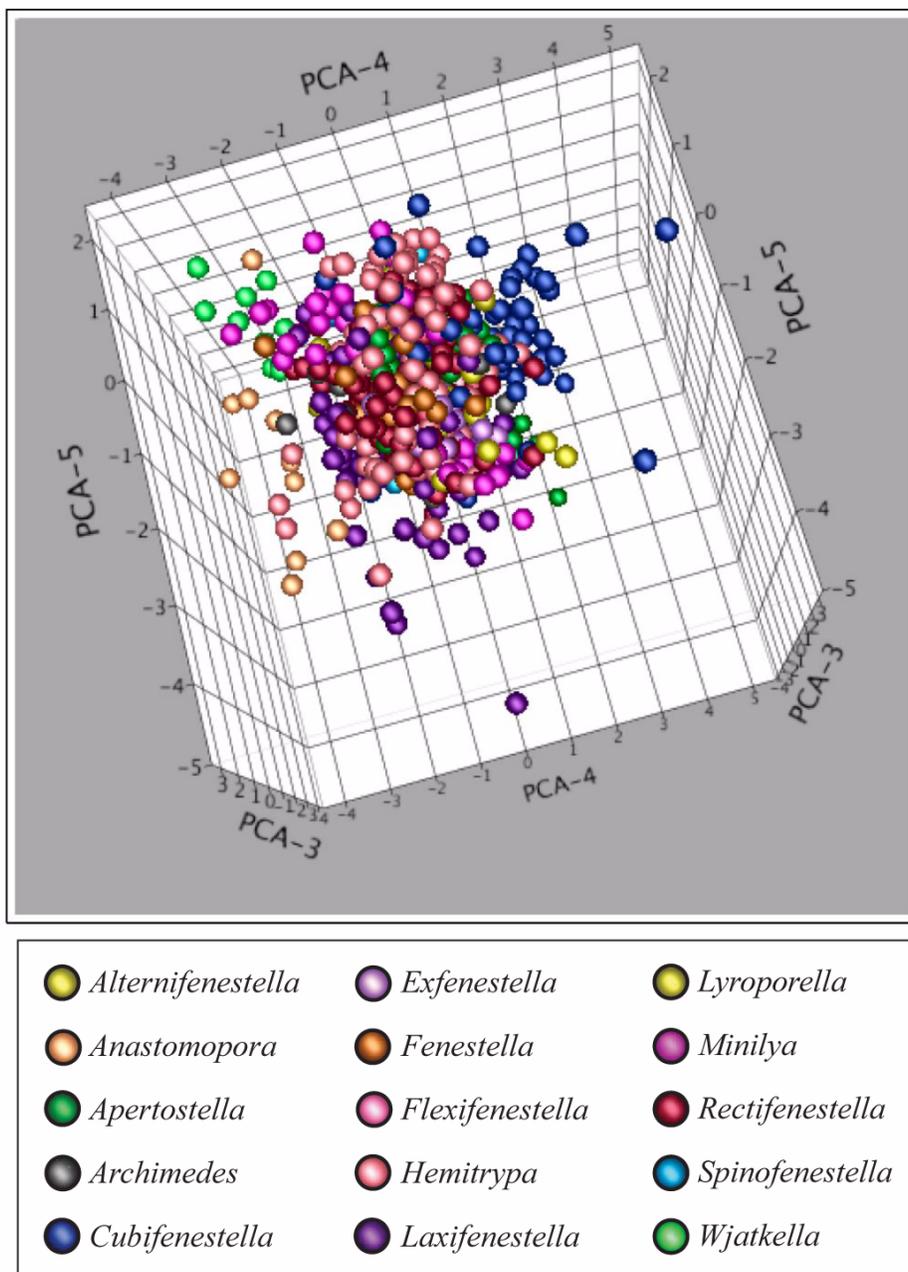
FIGURE 8. Scatter plot of all genera for PCA-3 vs. PCA-4 vs. PCA-5, which combined account for 28.7% of the variance. This view permits an evaluation of distributions along PCA-4 and PCA-5. Animation of the three axes in rotation is provided by Animation 2, which can also be accessed via the Animation Menu. Figure 7 is an orthogonal view (PCA-4 vs. PCA-5) of this image.

and apertures more distantly spaced laterally across a branch (ALB) plot high on PCA-5 (to top on Figure 7). Specimens with wide dissepiments, large nodes, and close aperture spacing along branches plot low on PCA-5 (to bottom on Figure 7). The distribution of samples on PCA-5 can also be evaluated on Figure 8. Although specimens are centered on a mean of zero for PCA-5 (Figure 7), considerable variation exists toward negative values on the axis (bottom on Figure 7). Some variation among genera is visible along PCA-5.

PCA-6: Branch Width and Node Size/Spacing vs. Dissepiments Width and Aperture Size/Spacing. Axis six reflects an inverse relationship
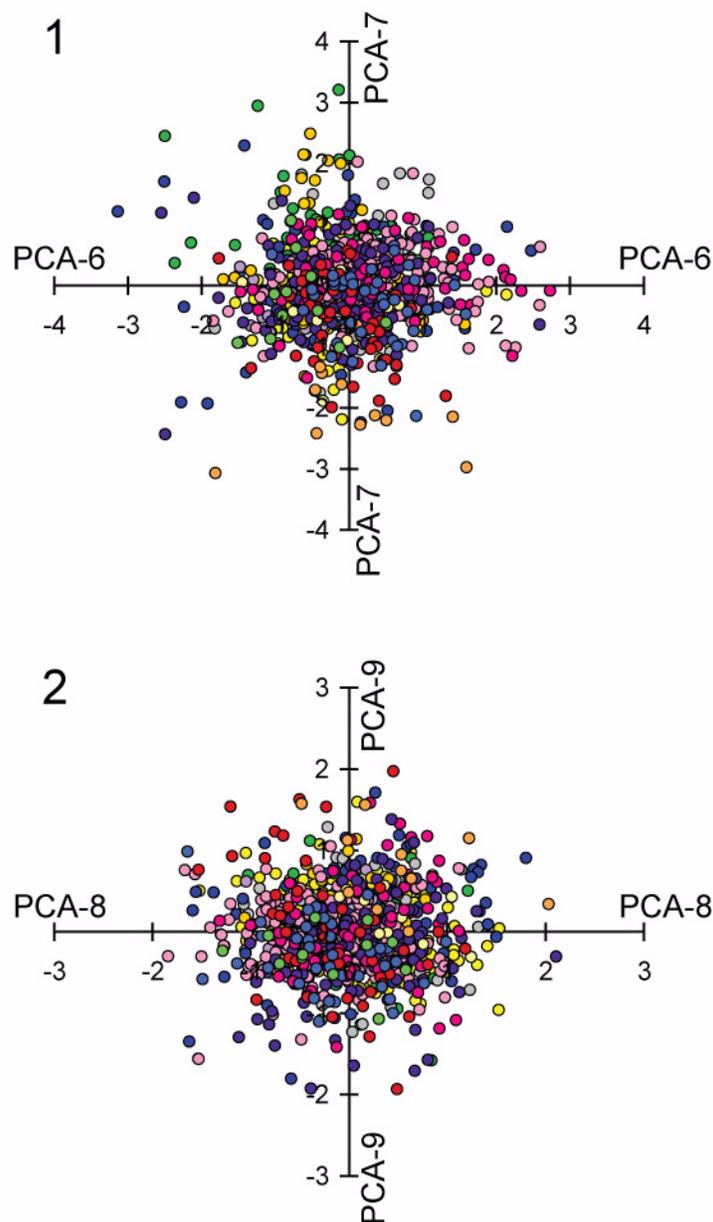
FIGURE 9. Scatter plot of principal components six through nine, which account for variation within genera (little discriminatory value among genera). (1) PCA-6 vs. PCA-7, which combined account for 11.2% of the total variance. PCA-6 reflects an inverse relationship between the width of dissepiments, lateral spacing and size of apertures vs. node size and spacing (Table 6). PCA-7 reflects an inverse relationship between the width of fenestrules and size of nodes vs. the spacing of nodes and spacing of apertures along branch (Table 6). Figure 10 is an inclined, three-dimensional view of this image. (2) PCA-8 vs. PCA-9, which combined account for 6.6% of the total variance. PCA-8 reflects an inverse relationship between the width of fenestrules and aperture spacing along branch vs. node diameter and lateral spacing of apertures across branch (Table 6). PCA-9 reflects an inverse relationship between the length of fenestrules vs. the spacing of nodes and lateral spacing of apertures across branch (Table 6).

between wider branches with larger, more distantly spaced nodes as compared to narrower dissepiments and with smaller more closely spaced apertures (Table 6). Specimens with wide dissepiments (DW) and larger more distantly spaced apertures (ALB and AD), plot high on PCA-6 (to right on Figure 9.1). Specimens with wide branches and large distantly spaced nodes plot low on PCA-6 (to left
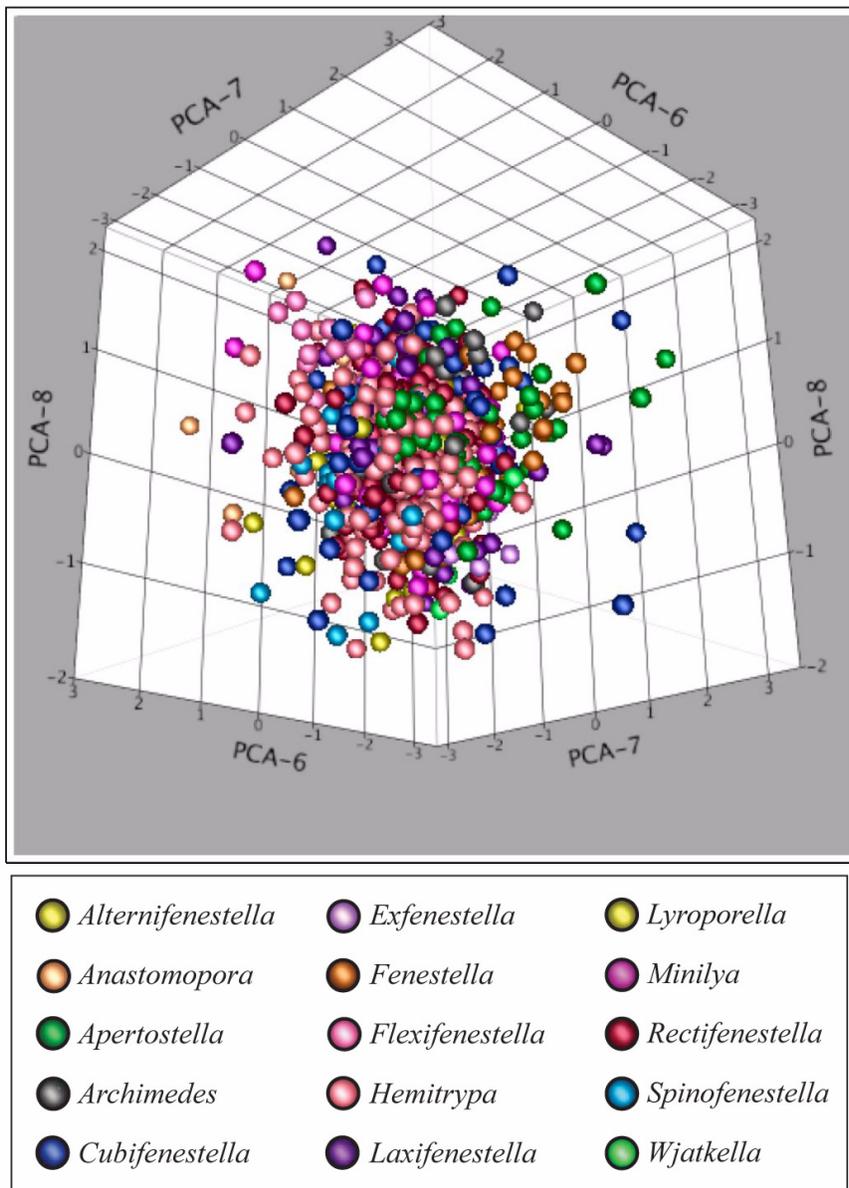
FIGURE 10. Scatter plot of all genera for PCA-6 vs. PCA-7 vs. PCA-8, which combined account for 14.8% of the variance. Animation of the three axes in rotation is provided by Animation 3, which can also be accessed via the Animation Menu. Figure 9.1 is an orthogonal view (PCA-6 vs. PCA-7) of this image.

on Figure 9.1). Although specimens are centered on a mean of zero for PCA-6, values are scattered from -3.0 to +3.0 on Axis six (Figure 9.1). The distribution of samples on PCA-6 can also be viewed on Figure 10.

PCA-7: Fenestrule Width and Node Diameter vs. Node and Aperture Spacing. Axis seven reflects an inverse relationship between wider fenestrules with larger nodes as compared to more closely spaced nodes and apertures (Table 6). Specimens with wide fenestrules (FW) and large nodes (ND), plot low on PCA-7 (to bottom of Figure 9.1). Specimens with more distantly spaced nodes (NS) and apertures along branch (AAB) plot high on PCA-7 (to top on Figure 9.1). Specimens are centered on a mean of zero for PCA-7, but values are scattered from -3.0 to +3.0 on Axis seven (Fig-

TABLE 4. Loading coefficients for each Principal Component Axis. Large absolute values reflect stronger correlation (importance) for a character on each axis. Blue highlights positive values on an axis (large original values plot high on axis), and red highlights negative values on an axis (large original values plot low on axis).

| Character Name | Principal Component Axis | | | | | | | | | Character Abbrev. |
	1	2	3	4	5	6	7	8	9	
Branch Width	**0.30**	-0.213	0.195	-0.622	0.102	-0.640	0.107	-0.082	0.004	BW
Dissepiment Width	**0.29**	-0.461	0.053	-0.328	-0.553	**0.498**	-0.105	0.166	-0.040	DW
Fenestrule Length	**0.40**	0.172	-0.452	-0.069	0.134	0.065	0.087	**0.274**	**0.706**	FL
Fenestrule Width	**0.39**	0.123	-0.369	-0.013	0.079	0.005	-0.648	-0.461	-0.242	FW
Aperture Diameter	**0.28**	-0.494	**0.311**	**0.296**	**0.492**	**0.252**	0.134	-0.362	**0.200**	AD
Aperture spacing Lateral across Branch	**0.37**	0.352	0.233	-0.150	**0.426**	**0.292**	0.064	**0.441**	-0.445	ALB
Aperture spacing Along Branch	**0.30**	**0.535**	**0.318**	0.009	-0.386	0.109	**0.350**	-0.478	0.112	AAB
Node Diameter	**0.32**	-0.002	**0.408**	**0.506**	-0.250	-0.362	-0.378	**0.349**	0.122	ND
Node Spacing	**0.34**	-0.206	**-0.447**	**0.367**	-0.160	**-0.214**	**0.512**	0.045	**-0.419**	NS

ure 9.1). The distribution of samples on PCA-7 can also be viewed on Figure 10.

PCA-8: Fenestrule Width and Aperture Size/ Spacing vs. Node Diameter, Fenestrule Length and Aperture Spacing. Axis eight reflects an inverse relationship between larger apertures more distantly spaced along branches and wider fenestrules as compared to more distantly spaced apertures laterally across branches, large nodes, and long fenestrules. Specimens with wide fenestrules (FW) and large apertures (AD) that are distantly spaced along branch (AAB), plot low on PCA-8 (to left of Figure 9.2). Specimens with large nodes (ND), long fenestrules (FL), and distantly spaced apertures laterally (ALB) plot high on PCA-8 (to right on Figure 9.2). Specimens are centered on a mean of zero for PCA-8, but values are restricted to only -2.0 to +2.0 on Axis eight (Figure 9.2). The distribution of samples on PCA-8 can also be viewed on Figure 10.

PCA-9: Node and Aperture Spacing and Fenestrule Width vs. Fenestrule Length and Aperture Diameter. Axis nine reflects a complex inverse relationship between more distantly spaced nodes and apertures as compared to narrower fenestrules with large apertures. Specimens with distantly spaced nodes (NS) and lateral spacing of apertures (ALB) and wide fenestrules (FW), plot low on PCA-9 (to bottom of Figure 9.2). Specimens

with long fenestrules and large apertures plot high on PCA-9 (to top on Figure 9.2).

Distribution of Genera in Morphospace

Fenestellid genera are compared here in a morphospace defined by the first three principal components, which account for 64.9% of variance and represent 1) overall size (small vs. large); 2) aperture spacing along branch vs. aperture size and dissepiment width (AD vs. AD, DW); and 3) node size, aperture spacing along branch and aperture diameter vs. fenestrule size and node spacing (ND, AAB vs. FL, FW, NS). Although axes four and five also represent among genera variance, trends are less general and are only reported in cases of relevance. In the following descriptions, "clouds" or "clusters" of OTUs are described in morphospace, but the values provided are intended to direct the reader's eye, not to provide absolute ranges for observed values (Table 7).

Data points (colony-level observations), color coded to represent the genera *Rectifenestella, Laxifenestella,* and *Fenestella*, are plotted on PCA-1 and PCA-3, and on PCA-2 and PCA-3 in Figure 11. These same data are plotted on PCA-1, PCA-2, and PCA-3 in Figure 12 with all data points from the study included as small black spheres for reference. Genera are highlighted in groups as *Rectifenestella* (Figure 12.1, axes animated in rotation in Animation 4); *Laxifenestella* and *Rectifenestella*

TABLE 5. Inverse relationships among characters for variation *among* genera. Summary from Table 4, with characters illustrated in Figure 2.

Principal Component Axis	Among Genera Potential inverse relationships shown across columns for each PCA	
PCA-1	All characters large	All characters small
PCA-2	Aperture spacing Along Branch (AAB)	Aperture Diameter (AD) Dissepiment Width (DW)
PCA-3	Node Diameter (ND) Aperture spacing Along Branch (AAB) Aperture Diameter (AD)	Fenestrule Length (FL) Node spacing (NS) Fenestrule Width (FW)
PCA-4	Node Diameter (ND) Node spacing (NS) Aperture Diameter (AD)	Branch Width (BW) Dissepiment Width (DW)
PCA-5	Aperture Diameter (AD) Aperture spacing Laterally across Branch (ALB)	Dissepiment Width (DW) Aperture spacing Along Branch (AAB) Node Diameter (ND)

(Figure 12.2, axes animated in rotation in Animation 5); *Fenestella, Laxifenestella,* and *Rectifenestella* (Figure 12.3, axes animated in rotation in Animation 6); and *Hemitrypa, Rectifenestella,* and *Lyroporella* (Figure 12.4, axes animated in rotation in Animation 7).

Data points, color coded to represent each genus in this study, are plotted in several combinations on PCA-4 and PCA-5 in Figure 13. Combinations of genera included in Figure 13 are 1) *Rectifenestella*, *Laxifenestella* and *Fenestella*; 2) *Rectifenestella*, *Hemitrypa,* and *Lyroporella*; 3) *Rectifenestella*, *Fenestella,* and *Archimedes*; 4) *Rectifenestella*, *Cubifenestella,* and *Apertostella*; 5) *Alternifenestella*, *Minilya,* and *Spinofenestella*; and 6) *Exfenestella*, *Flexifenestella*, *Anastomopora,* and *Wjaktella*.

Data points, color coded to represent the genera in groups of *Archimedes, Fenestella,* and *Rectifenestella*, and *Cubifenestella, Apertostella,* and

Rectifenestella, are plotted on PCA-1 and PCA-3, and on PCA-2 and PCA-3 in Figure 14. The data for these two groups of genera are plotted on PCA-1, PCA-2, and PCA-3 in Figure 15. The group that highlights *Archimedes* (Figure 15.1) has axes animated in rotation in Animation 8. The group that highlights *Cubifenestella* and *Apertostella* (Figure 15.2) has axes animated in rotation in Animation 9).

Data points, color coded to represent the genera, grouped as 1) *Alternifenestella, Minilya,* and *Spinofenestella* and 2) *Exfenestella, Flexifenestella, Anastomopora,* and *Wjaktella*, are plotted on PCA-1 and PCA-3 and on PCA-2 and PCA-3 in Figure 16. The first group of data (Figure 16.1) has axes animated in rotation in Animation 1), and the second group (Figure 15.2) has axes animated in rotation in Animation 1.

Rectifenestella. The genus *Rectifenestella* Morozova, 1974 was originally diagnosed as a fenestel-

TABLE 6. Inverse relationships among characters for variation *within* genera (potentially among species, among colonies, within colonies and residual). Summary from Table 4 with characters illustrated in Figure 2.

Principal Component Axis	Within Genera Potential inverse relationships shown across columns for each PCA	
PCA-6	Dissepiment Width (DW)	Branch Width (BW)
	Aperture spacing Laterally across Branch (ALB)	Node Diameter (ND)
	Aperture Diameter (AD)	Node Spacing (NS)
PCA-7	Node Spacing (NS)	Fenestrule Width (FW)
	Aperture spacing Along Branch (AAB)	Node Diameter (ND)
PCA-8	Aperture spacing Laterally across Branch (ALB)	Aperture spacing Along Branch (AAB)
	Node Diameter (ND)	Fenestrule Width (FW)
	Fenestrule Length (FL)	Aperture Diameter (AD)
PCA-9	Fenestrule Length (FL)	Aperture spacing Laterally
	Aperture Diameter (AD)	Node Spacing (NS)
		Fenestrule Width (FW)

lid having straight branches and dissepiments, pentagonal cross sections of endozonal zooecial chambers, and a single series of keel nodes (Morozova 1974). It was chosen as the fenestellid genus for standard of comparison here because of its basic form, large number of observations (243), and number of nominal species (seven) widely scattered both stratigraphically and geographically (Appendix). The distribution of *Rectifenestella* in morphospace can be summarized as follows.

1. On Figure 11.1 there is a highly coherent cluster to the left side almost centered on PCA-3 (PCA-1 values from -2.5 to 0.0 and PCA-3 values from -2. to 2.0). The cluster is bounded on the right by a sharp boundary (PCA-1 0.0) and tapers to the left converging on PCA-1 and PCA-3 values of -3.0 and -0.5.

2. On Figure 11.2 there is a coherent cluster centered to the right of the origin (0.5, 0.5) with a range of PCA-2 values from -2.0 to 2.0 and PCA-3 values from -2.0 to 2.0).

3. On Figure 13.1 there is a single, coherent cluster centered on the origin (PCA-4 values from -1.0 to 1.0 and PCA-5 values from -1.5 to 1.5).

Laxifenestella. The genus *Laxifenestella* Morozova, 1974 was originally diagnosed as a fenestellid having straight to slightly sinuous branches, moderately broad dissepiments, well-developed superior hemisepta, tetragonal to pentagonal cross sections of endozonal zooecial chambers, and small, closely spaced keel nodes (Morozova 1974). It is represented here by a large number of observations (117) and six nominal species with broad geographic and stratigraphic distribution. The distribution of *Laxifenestella* in morphospace falls into two discrete subclusters and can be summarized as follows.

1. On Figure 11.3 there is a tight subcluster in the upper left quadrant (PCA-1 values from -2.0 to -1.0 and PCA-3 values from 0.5 to 1.5). A second, more diffuse subcluster is found in the right region centered on PCA-3 (PCA-1 values from 0.0 to 4.0 and PCA-3 -2.0 to 1.5). The first subcluster (all OTUs assigned to *Laxifenestella serratula* (Ulrich) by Snyder (1991)) coincides with observations from *Fenestella* and *Rectifenestella*.

2. On Figure 11.4 there is a single, diffuse cluster centered on the origin (PCA-2 values from

TABLE 7. Summary of characters, and for which Principal Component Axis they are most important, i.e., how large absolute values for measures are expressed on selected axes. "Low" indicates a negative loading coefficient, plotting low on the PCA axis, and "high" the opposite. Characters are ordered by their relative importance (absolute value of loading coefficients, Table 4) to among genera variation and are illustrated in Figure 2.

Character	Variation Among Genera	Variation Within Genera
Aperture Diameter (AD)	PCA-2 (low)	variable
	PCA-3 (high)	
	PCA-5 (high)	
Dissepiment Width (DW)	PCA-2 (low)	PCA-6 (high)
	PCA-5 (low)	
Aperture Along-Branch spacing (AAB)	PCA-2 (high)	PCA-8 (low)
Node Diameter (ND)	PCA-3 (high)	PCA-8 (high)
	PCA-4 (high)	
Fenestrule Length (FL)	PCA-3 (low)	PCA-9 (high)
Fenestrule Width (FW)	PCA-3 (low)	PCA-7 (low)
Node Spacing (NS)	PCA-3 (low)	PCA-7 (high)
		PCA-9 (low)
Aperture Lateral	PCA-3 (high)	PCA-8 (high)
Spacing (ALB)	PCA-5 (high)	
Branch Width (BW)	PCA-4 (low)	PCA-6 (low)

-2.0 to 2.0 and PCA-3 values from -2.0 to 1.5).

3. On Figure 13.1 there is a single diffuse cluster centered on the lower left quadrant (PCA-4 values from -2.0 to 1.5 and PCA-5 values from -2.5 to 1.5).

Fenestella. The genus *Fenestella* Lonsdale, 1839, was the second fenestrate genus named, for zoaria "composed of branches which unite by growth and form a cup," characterized by "one row" of zooecia on branches and none on branch interconnections. It is the most well known and misapplied fenestellid genus name. It is represented here by 60 observations from five nominal species. The distribution of *Fenestella* in morphospace falls into two discrete subclusters and can be summarized as follows.

1. On Figure 11.5 there is a tight subcluster in the lower left quadrant (PCA-1 values from -3.0 to -2.0 and PCA-3 values from -2.0 to -1.0). The first subcluster is comprised entirely of OTUs from specimens assigned to *Fenestella* sp. 1 in Ernst and Schroeder (2007). A second, more diffuse subcluster is found in the central region (PCA-1 values from -0.5 to 1.5 and PCA-3 -3.0 to 2.0). The second subcluster forms a relatively tight disk-shaped cloud, which falls in a zone between *Rectifenestella* and *Laxifenestella*.

2. On Figure 11.6 there is a single, diffuse cluster to the left side (PCA-2 values from -2.0 to 0.0 and PCA-3 values from -3.0 to 2.0). Unlike observations for the previous two genera, *Fenestella* is restricted to a negative distribution on PCA-2.

3. On Figure 13.1 there is a single cluster centered on the origin (PCA-4 values from -1.5 to 1.0 and PCA-5 values from -1.0 to 1.5).

Hemitrypa. The genus *Hemitrypa* Phillips, 1841 was named for fenestrate bryozoans with a fine-textured side that proved to be a finely reticulate superstructure with each opening in the superstructure centered over a single zooecial aperture. It is represented here by 225 observations from nine nominal species. In morphospace (Figures 14.1–14.2, 12.4), *Hemitrypa* observations form a relatively cohesive cloud that has a complex
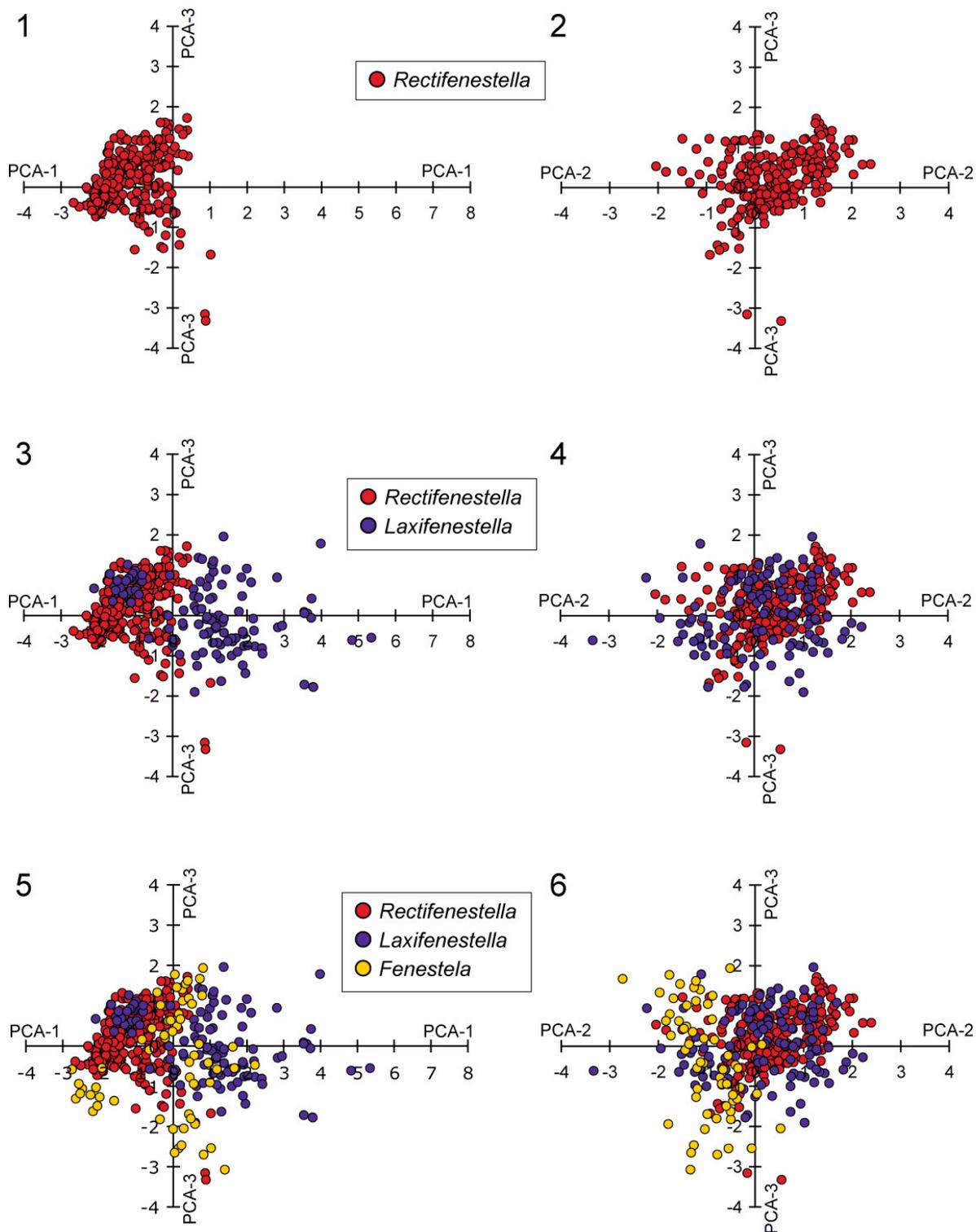
FIGURE 11. Scatter plots of observations by genus (*Rectifenestella*, *Laxifenestella* and *Fenestella*) on (1, 3, 5) PCA-1 vs. PCA-3 and (2, 4, 6) PCA-2 vs. PCA-3. See Figure 12.1 for three-dimensional animation with *Rectifenestella* highlighted. See Figure 12.2 for three-dimensional animation with *Laxifenestella* highlighted. See Figure 12.3 for three-dimensional animation with *Fenestella* highlighted.
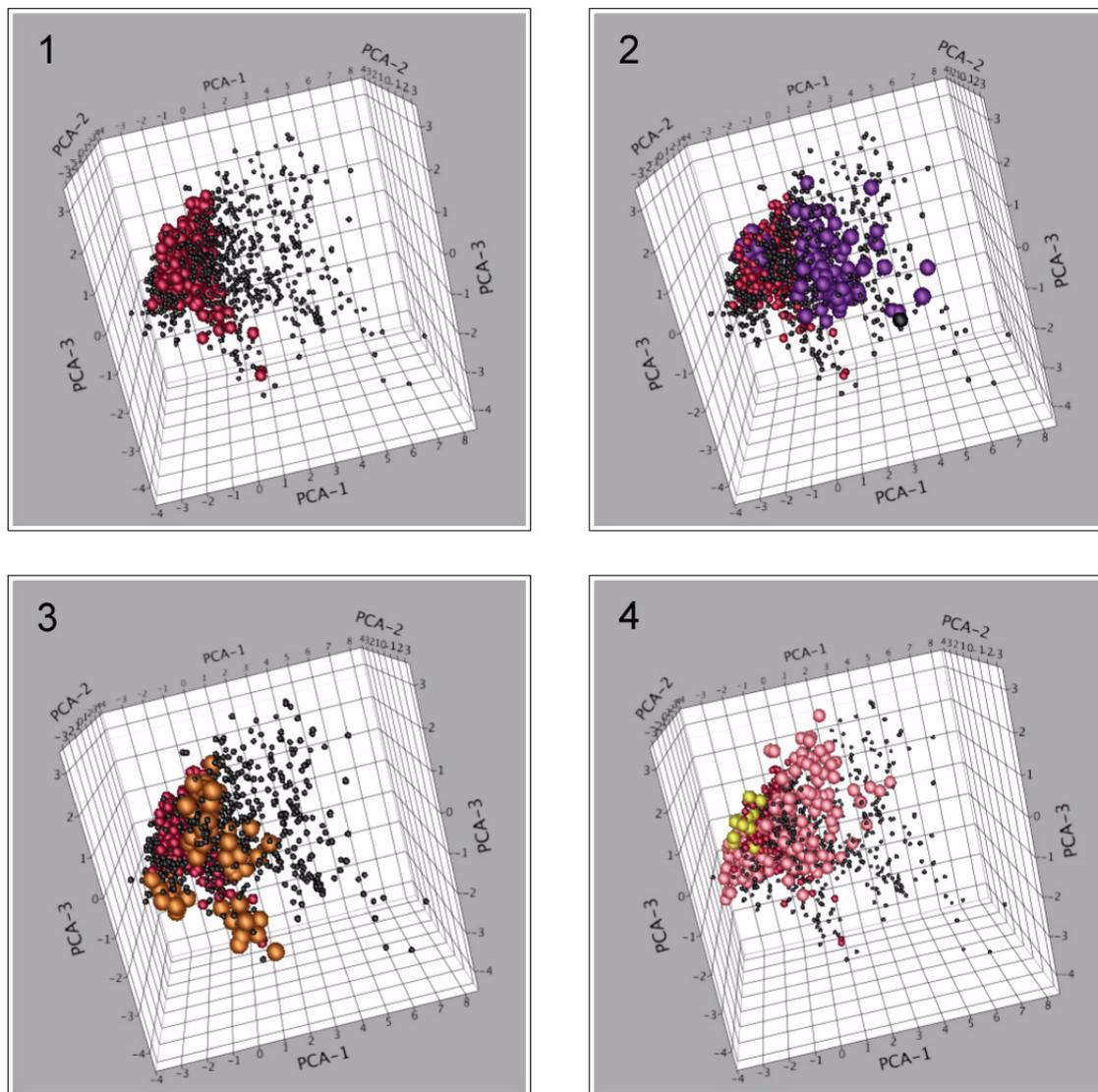
FIGURE 12. Three dimensional, rotating scatter plots of PCA-1 vs. PCA-2 vs. PCA-3 by genus. (1-4) *Rectifenestella* (red) with other, non-highlighted fenestrate genera in black. (1) Animation of the three axes in rotation is provided by Animation 4 for *Rectifenestella*. (2) *Laxifenestella* highlighted in purple, with animation of axes in rotation provided by Animation 5; (3) *Fenestella* highlighted in bronze, with animation of axes in rotation provided by Animation 6; and (4) *Hemitrypa* highlighted in pink and *Lyroporella* highlighted in yellow, with animation of axes in rotation provided by Animation 7. All animations are accessible via the Animation Menu.

shape. The distribution of *Hemitrypa* in morphospace can be summarized as follows.

1. On Figure 14.1 there is a coherent, conical cluster centered on the origin, with a pronounced taper toward the lower left quadrant converging on values of PCA-1 and PCA-3 of -3.0 and -1.0. The range of values on PCA-1 is from -3.0 to 4.0 and PCA-3 is -1.0 to 3.0. There is a horizontal boundary at PCA-3 of -1.0. The overall size of measured characters

ranges from some of the smallest observations (Figure 14.1, value of -3.5 on PCA-1) to mid-sized including the range for *Rectifenestella*, *Fenestella,* and *Laxifenestella*. As the overall size of observed *Hemitrypa* increases, values extend preferentially into the upper right quadrant of Figure 14.1.

2. On Figure 14.2 there is a coherent cloud extending from the center to the upper left quadrant, with PCA-2 values from -2.0 to 1.0
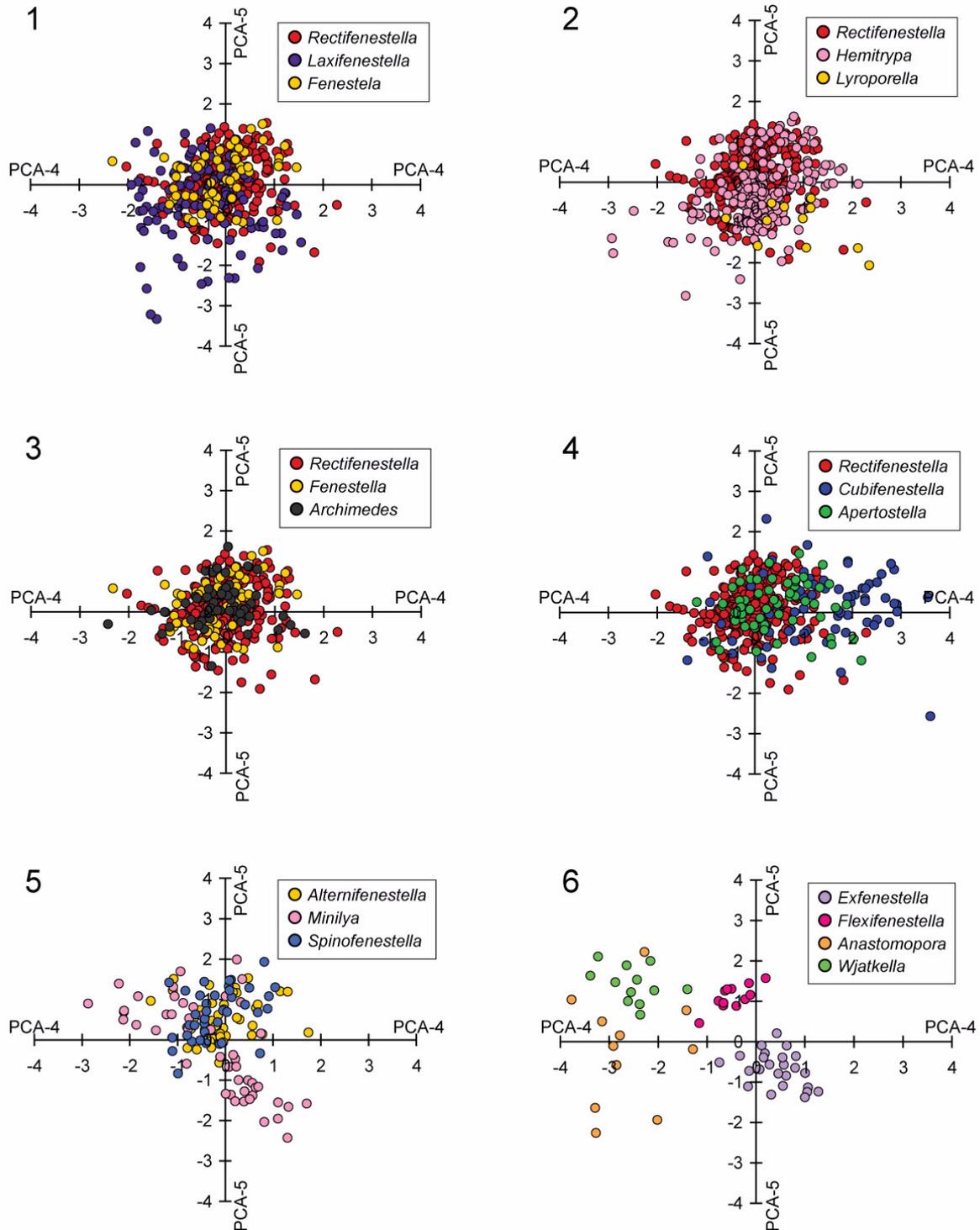
FIGURE 13. Scatter plots of observations by genus on PCA-4 vs. PCA-5 for all genera.
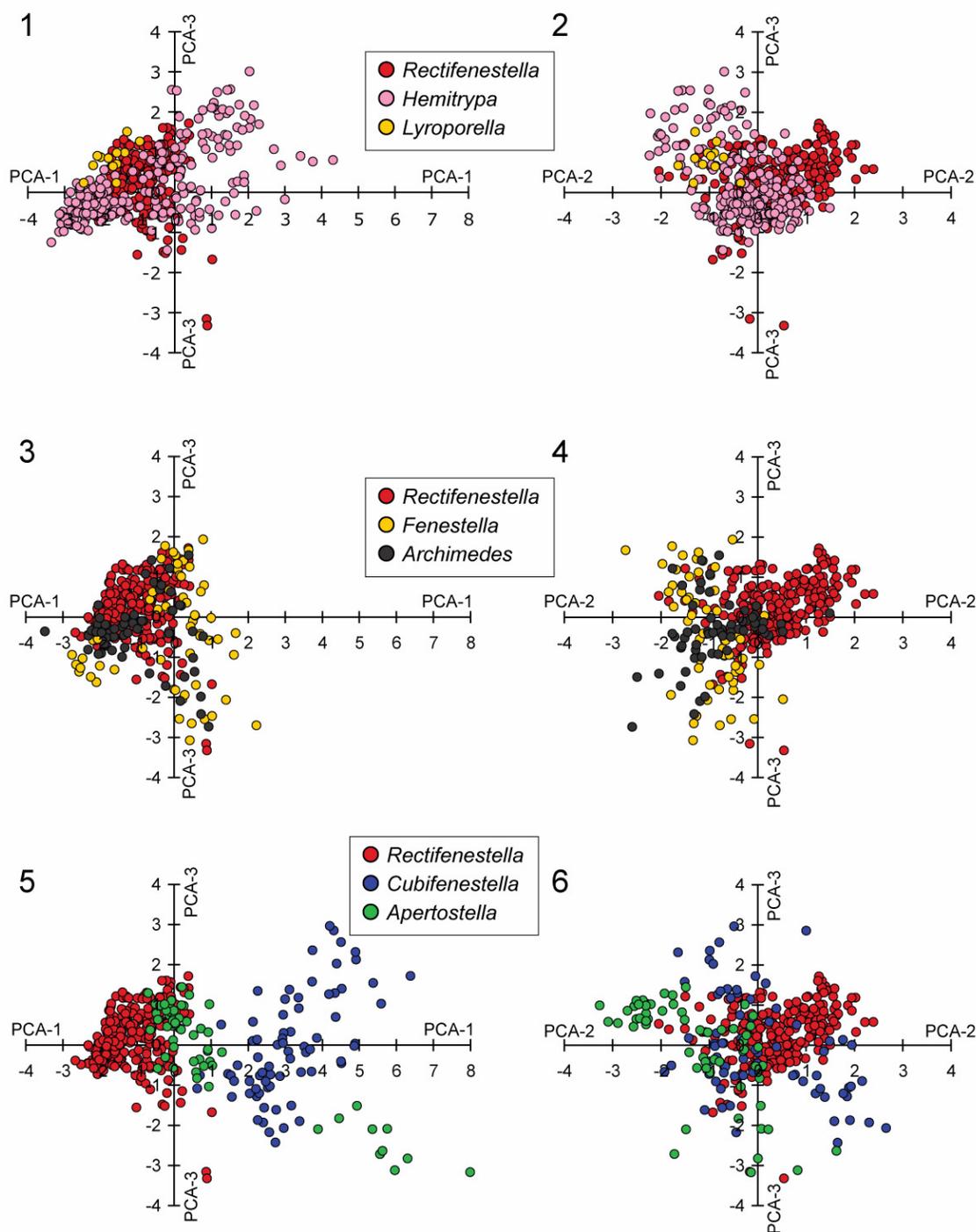
FIGURE 14. Scatter plots of observations by genus on (1, 3, 5) PCA-1 vs. PCA-3; and (2, 4, 6) PCA-2 vs. PCA-3. (1, 2) *Rectifenestella*, *Hemitrypa,* and *Lyroporella* (see Figure 12.4 for three-dimensional animation); (3, 4) *Archimedes*, *Rectifenestella,* and *Fenestella* (see Figure 15.1 for three-dimensional animation); and (5, 6) *Cubifenestella*, *Apertostella,* and *Rectifenestella* (see Figure 15.2 for three-dimensional animation).

and PCA-3 values from -1.0 to 3.0.

3. On Figure 13.2 there is a coherent, somewhat diffuse cloud centered on the origin with PCA-4 values from -3.0 to 2.0 and PCA-5 values

from -3.0 to 1.5.

Archimedes. The genus *Archimedes* Owen, 1838 was the earliest Paleozoic fenestrate genus established, characterized and named on the basis of its
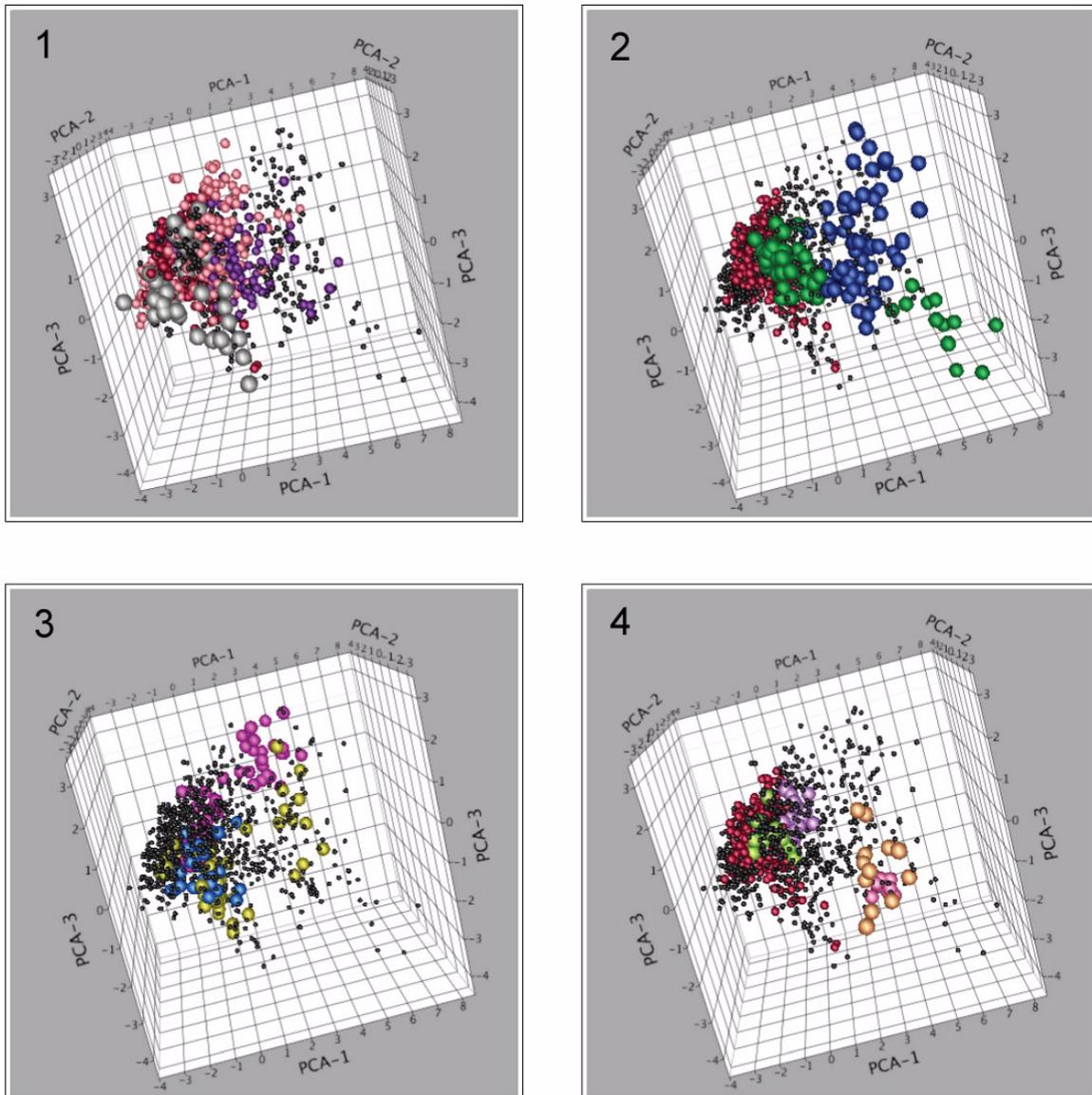
FIGURE 15. Three-dimensional, rotating scatter plots of PCA-1 vs. PCA-2 vs. PCA-3 by genus. (1) *Archimedes* highlighted in large silver spheres, *Rectifenestella* (red), *Laxifenestella* (purple), *Hemitrypa* (pink), with other non-highlighted fenestrate genera in black. Rotation of axes is provided by Animation 8. (2) *Cubifenestella* highlighted in blue and *Apertostella* highlighted in green, with *Rectifenestella* in red and other genera in black. Rotation of axes is provided by Animation 9. (3) Scatter plot that includes *Alternifenestella* (gold), *Minilya* (pink), and *Spinofenestella* (blue). Rotation of axes is provided by Animation 10. (4) Scatter plot that includes *Exfenestella* (purple), *Flexifenestella* (pink), *Anastomopora* (tan), and *Wjatkella* (green). Rotation of axes is provided by Animation 11. All animations are accessible via the Animation Menu.

helical support structure. It is represented here by 60 observations from five nominal species. The distribution of *Archimedes* in morphospace can be summarized as follows.

1. On Figure 14.3 there is a coherent cluster to the left side almost centered on PCA-3 (PCA-1 values from -2.5 to 1 and PCA-3 values from -3.0 to 1.5). The cluster is bounded on the right by an inclined boundary (PCA-1 0.5 to 1.0) and tapers to the left converging on PCA-1 and PCA-3 values of -2.0 and -1.0. *Archimedes* occupies a range of morphospace similar
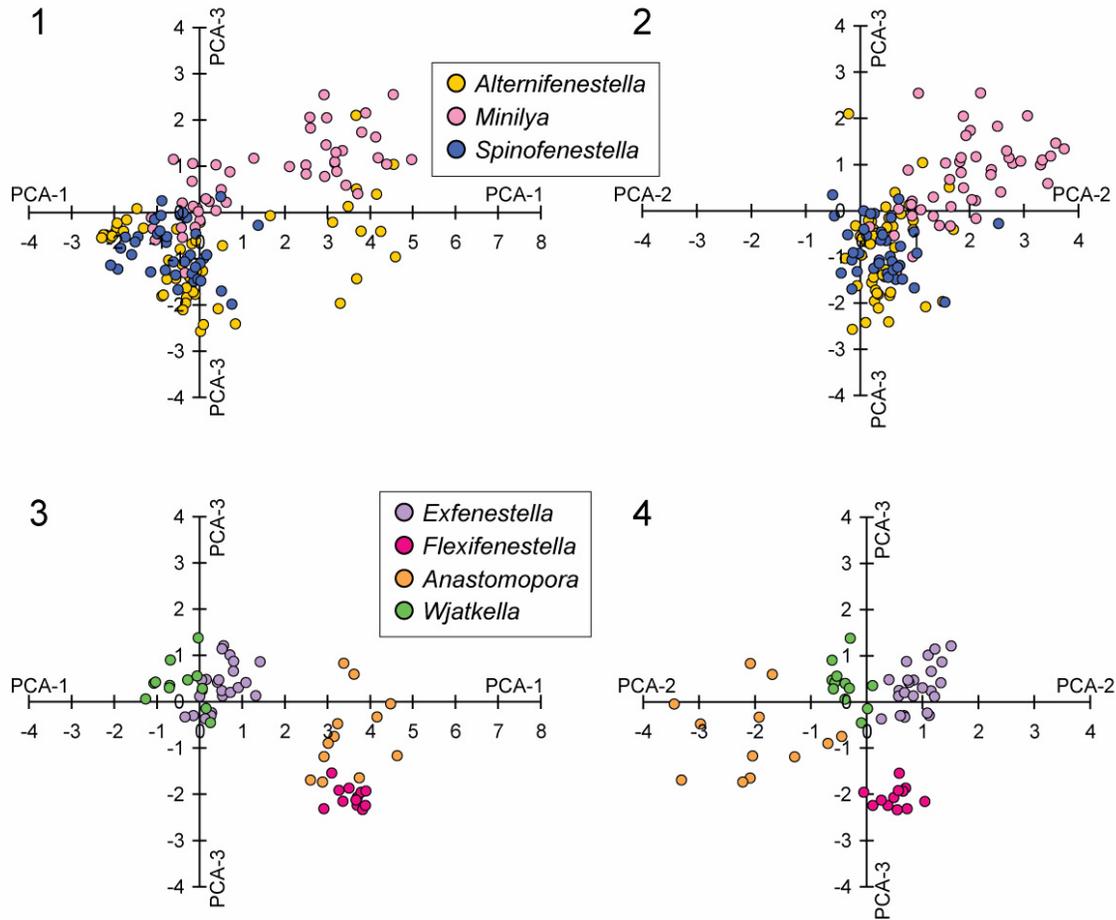
FIGURE 16. Scatter plots of observations by genus on (1, 3) PCA-1 vs. PCA-3; and (2, 4) PCA-2 vs. PCA-3. (1, 2) *Spinofenestella, Alternifenestella,* and *Minilya* (see Figure 15.3 for three-dimensional animation); and (3, 4) *Exfenestella*, *Flexifenestella, Anastomopora,* and *Wjatkella* (see Figure 15.4 and Animation 11).

to *Rectifenestella* and *Fenestella*.

2. On Figure 14.4 there is a coherent cluster located largely to the left of the origin (-1.0, -0.5) with a range of PCA-2 values from -2.0 to 0.5 and PCA-3 values from -3.0 to 1.5). As the overall size of *Archimedes* features increase, the observations are largely restricted to the negative regions of PCA-2 (to the left on Figure 14.4).

3. On Figure 13.3 there is a single diffuse cluster centered on the origin (PCA-4 values from -1.5 to 1.5 and PCA-5 values from -0.5 to 1.5).

Cubifenestella. The genus *Cubifenestella* Snyder, 1991 was originally diagnosed as a fenestellid having robust zoarial meshwork and several internal characters including absence of hemisepta, intermediate chamber size, and cubic to irregularly rectangular endozonal zooecial chambers (Snyder 1991). It is represented here by 72 observations

from three nominal species. The distribution of *Cubifenestella* in morphospace can be summarized as follows.

1. On Figure 14.5 there is a diffuse but coherent cluster in the right side almost centered on PCA-3 (PCA-1 values from 1.5 to 6 and PCA-3 values from -2.5 to 3.0).

2. On Figure 14.6 there is a diffuse cluster centered on the origin (PCA-2 values from -2.0 to 2.5 and PCA-3 values from -2.5 to 3.0).

3. On Figure 13.4 there is a single, tight cluster to the right, centered on PCA-5 (PCA-4 values from -1.0 to 3.0 and PCA-5 values from -1.5 to 1.5).

Apertostella. The genus *Apertostella* Snyder, 1991 was originally diagnosed as a fenestellid having delicate to robust meshwork characteristics and a complex of internal characteristics including inter-

mediate endozonal chamber and zooecial aperture size, no hemisepta, and rectangular box shaped endozonal zooecial chambers (Snyder 1991). The genus as represented by the specimens at hand does not form a coherent cluster. The distribution of *Apertostella* in morphospace can be summarized as follows.

1. On Figure 14.5 there is a tight subcluster centered on the origin (PCA-1 values from -1.0 to 1.0 and PCA-3 values from -1.0 to 1.5). This subcluster occupies morphospace shared by *Fenestella*. A second, more diffuse subcluster is found in the lower right quadrant (PCA-1 values from 4.0 to 8.0 and PCA-3 values from -3.0 to -1.5). The second subcluster consists of OTUs entirely from specimens assigned to the species *Apertostella venusta* Snyder, 1991. The second subcluster of *Apertostella* occupies morphospace independent of any other fenestellid genus, but adjacent to *Cubifenestella.*

2. On Figure 14.6 there is a single, diffuse cluster to the left (PCA-2 values from -3.5 to 1.0 and PCA-3 values from -3.0 to 1.5).

3. On Figure 13.4 there is a single diffuse cluster slightly offset into the upper right quadrant (PCA-4 values from -1.0 to 2.0 and PCA-5 values from -1.0 to 1.5).

Data points, color coded to represent the genera in groups of 1) *Aternifenestella*, *Minilya,* and *Spinofenestella*; and 2) *Exfenestella, Flexifenestella, Anastomopora* and *Wjatkella* are plotted on PCA-1 and PCA-3 and on PCA-2 and PCA-3 in Figure 16. These same data are plotted on PCA-1, PCA-2 and PCA-3 in Figure 15, with all data points in the study included for reference as small black spheres. Frames of Figure 15 are linked to animations of the axes in rotation.

Minilya. The genus *Minilya* Crockford, 1944 was originally diagnosed as a fenestellid having small keel nodes in two alternating rows and having subtriangular cross sections of endozonal zooecial chambers. It is represented here by 24 observations from two nominal species. The distribution of *Minilya* in morphospace can be summarized as follows.

1. On Figure 16.1 there is a diffuse, elongate cloud extending into the upper right quadrant (PCA-1 values from -1.0 to 5.0 and PCA-3 values from -0.5 to 2.5).

2. On Figure 16.2 there is a diffuse, elongate cloud in the upper right quadrant (PCA-2 val-

ues from 0.0 to 4.0 and PCA-3 values from -0.5 to 2.5).

3. On Figure 13.5 there is a coherent, diffuse cluster inclined from the upper left to lower right quadrants (PCA-4 values from -2.5 to 2.0 and PCA-5 values from -2.5 to 2.0).

Spinofenestella. The genus *Spinofenestella* Termier and Termier, 1971, was originally diagnosed as a fenestellid having a regular zoarial meshwork of short fenestrules, with a zooecial aperture at the base of each dissepiment and a single row of keel nodes (Termier and Termier 1971). It is represented by 38 observations from four nominal species. The distribution of *Spinofenestella* in morphospace can be summarized as follows.

1. On Figure 16.1 there is single cloud centered in the lower left quadrant (PCA-1 values from -2.0 to 1.5 and PCA-3 values from -2.0 to 0.5). Observations largely overlap the morphospace occupied by a subcluster of *Alternifenestella.*

2. On Figure 16.2 there is a coherent cloud centered in the lower right quadrant (PCA-2 values from -0.5 to 1.0 and PCA-3 values from -2.0 to 0.5).

3. On Figure 13.5 there is a single, coherent cloud in the upper central region (PCA-4 values from -1.0 to 1.0 and PCA-5 values from -1.0 to 2.0).

Alternifenestella. The genus *Alternifenestella* Termier and Termier, 1971 was not originally diagnosed, being valid only because a type species was designated for it (Termier and Termier 1971). Morozova (1974) diagnosed it as a fenestellid having thin straight branches and dissepiments, triangular to trapezoidal cross sections of endozonal zooecial chambers, frequently budded in a single row, and with a single series of keel nodes. It is represented here by 50 observations from five nominal species. The distribution of *Alternifenestella* in morphospace is also somewhat enigmatic and can be summarized as follows.

1. On Figure 16.1 there is a tight subcluster in the lower left quadrant (PCA-1 values from -2.0 to 1.0 and PCA-3 values from -2.0 to 0.0). A second, more diffuse subcluster is found in the right region centered on PCA-1 (PCA-1 values from 3.0 to 5.0 and PCA-3 -2.0 to 2.0). The first subcluster coincides with observations from the genus *Spinofenestella.*

2. On Figure 16.2 there is a single, tight cloud in the lower right quadrant (PCA-2 values from

TABLE 8. Covariance matrix for standardized data set used in principal components analysis. Abbreviations for characters defined in Figure 2. Lower half of matrix is covariance between characters. Upper half of the matrix lists probabilities that the null hypothesis that the two characters are uncorrelated (all p 0.0001, except AD (Aperture Diameter) and AAB (Aperture spacing Along Branch). Color highlights denote character groups with stronger covariance (except orange, which indicates exceptionally low).

	BW	DW	FL	FW	AD	ALB	AAB	ND	NS
BW	*	0.0000	0.0000	0.0000	0.0000	0.0000	0.0000	0.0000	0.0000
DW	0.41	*	0.0000	0.0000	0.0000	0.0000	0.0000	0.0000	0.0000
FL	0.33	0.29	*	0.0000	0.0000	0.0000	0.0000	0.0000	0.0000
FW	0.31	0.31	0.65	*	0.0000	0.0000	0.0000	0.0000	0.0000
AD	0.29	0.34	0.21	0.23	*	0.0000	0.0207	0.0000	0.0000
ALB	0.37	0.20	0.51	0.45	0.32	*	0.0000	0.0000	0.0000
AAB	0.22	0.17	0.35	0.31	0.07	0.53	*	0.0000	0.0000
ND	0.23	0.25	0.25	0.34	0.40	0.36	0.41	*	0.0000
NS	0.21	0.32	0.55	0.46	0.34	0.21	0.19	0.34	*

0.0 to 1.0 and PCA-3 values from -2.5 to 1.0), which coincides with observations from the genus *Spinofenestella*.

3. On Figure 13.5 there is a single, tight cloud in upper region centered on PCA-4 (PCA-4 values from -1.0 to 1.0 and PCA-5 values from 0.0 to 1.5). This cloud coincides with observations from the genus *Spinofenestella*.

Other Genera. Five additional genera are represented by single species. Among these the species of *Exfenestella* Morozova, 1974 and *Wjatkella* Morozova, 1970 are centrally placed within the total cloud, with the centroid of their respective clouds plotting near zero on PCA-1, PCA-2, and PCA-3 (Figure 16.3-16.4). These two genera therefore occupy portions of morphospace shared with *Rectifenestella*, *Fenestella,* and *Laxifenestella* (Figures 16.3–16.4, 15.4). Observations of *Flexifenestella* Morozova 1974 form a tight cloud in the lower right quadrant of Figure 16.3 and plot slightly positive on PCA-2 (Figure 16.4), and negative on PCA-3 (Figure 16.3-16.4).

The multiserial genus *Anastomopora* Simpson, 1897 forms a diffuse but coherent cloud centered on the right central region of Figure 16.3 and left central region of Figure 16.4 in the range of morphospace occupied by *Cubifenestella* and in part by *Apertostella*.

The genus *Lyroporella* Simpson, 1895 is a distinctive genus characterized by transversely arched ("lyre-shaped") zoaria that are weighted by thick skeletal deposits along the proximolateral margins. It was distinguished from polyporid lyre-

shaped species with multiple zooecial rows by having only two rows of zooecia that only increase to three rows proximal to branch bifurcations. Data here are restricted to 12 observations from a single nominal species. In morphospace (Figures 14.1-14.2, 12.4), *Lyroporella* observations plot in a compact cloud in the upper left quadrant of Figure 14.1-14.2, in a portion of the morphospace shared by *Rectifenestella* and *Hemitrypa*.

Relationships Among Morphometric Characters

The covariance between each pair of characters is highly significant (Table 8), except for AD-ABB, which is marginally significant. Several groups of characters show a greater degree of linkage (Table 8, highlighted by color).

1. FL-FW-ALB-NS: fenestrule size (length and width), Aperture spacing Laterally across Branch, and Node Spacing display the highest pair-wise covariance.

2. AAB-ALB-ND: spacing of apertures along branch and laterally as well as node size display moderately high pair-wise covariance.

3. BW-DW: branch width and dissepiment width display strong covariance.

4. AD-ND: aperture size and node size display moderately strong covariance.

5. Only the combination of aperture size (AD) and spacing of apertures along branch (AAB) displays a covariance notably lower than the rest of the pair-wise comparisons (Table 8).

DISCUSSION

Subdivision of the bryozoan genus *Fenestella* into several genera during the past half century raises the question of whether these genera 1) represent biological entities (individual or paraphyletic clades) or 2) are concepts of convenience that divide a continuum of morphologies involving independent repetitive evolution of artificially defined, plastic character states. With few exceptions, discussed below, the recently defined genera were initially differentiated on the basis of zooecial endozonal (interior) morphologies, geometric relationships among zooecia in the endozone, or consistent presence of unique heterozooecia, which are *not* among the nine exterior characters used in this analysis.

In this study, we have addressed the question of whether fenestellid genera as currently used have overall morphological coherence independent, or largely independent, of the initially defining characters, or whether instead species assigned to a genus plot in morphospace independently of one another. To do this we have used nine quantitatively variable characters that can be observed on the colony surface (Figure 2) and that generally were not part of the basis for naming the genera.

The relatively recently named genera, and a small number of genera named earlier and used as conceptual controls, each occur within only a portion of the occupied morphospace as defined by principal components of the nine quantifiable surface characters. Some genera in the study are represented by a single species, and each of these species is limited to a small portion of the occupied morphospace. This pattern is to be expected, inasmuch as elements of size and proportions are typical for discrimination of fenestrate bryozoan species within a genus. In addition, each genus that is represented by two or more species in the study also has a limited range of sizes of externally observable characters that – with one exception – differentiates it from other genera in the study.

Genera Originally Diagnosed in Part on One or More of the Nine Characters Used in This Study

Five of the included genera (*Alternifenestella*, *Cubifenestella*, *Laxifenestella*, *Minilya*, and *Spinofenestella*, Table 9) each had one or more elements of size of the meshwork or features seen on branch surfaces embodied in the original diagnosis. Elements of size were an important part of the characterization of *Cubifenestella* when it was named, but size was less emphasized in defining the other four genera. Nevertheless, it is worth

examining the apparent effect of the initially mentioned size element(s) in positioning each of these genera in morphospace.

Alternifenestella. The externally observable size characteristics included in the first diagnosis (Morozova 1974) of *Alternifenestella* Termier and Termier, 1971 were narrow branches and narrow dissepiments. Branch width (BW) does not appear in Table 9 as an important PCA loading coefficient on any of the axes for *Alternifenestella*. Dissepiment width (DW) does plot small on PCA-2 and PCA-5 for *Alternifenestella* (to the top on Figure 13.5 and to the right on Figure 16.2, and Table 9), but the magnitude of the loading coefficient is not dominant relative to other important characters (Table 4).

Cubifenestella. The original diagnosis of this genus noted intermediate to robust zoaria, with open mesh spacing based on intermediate to large fenestrules, with narrow to intermediate branch width and intermediate dissepiment width (Snyder 1991). Indeed *Cubifenestella* does plot entirely in the positive area of PCA-1 (Figure 14.5), confirming Snyder's concept of its general robustness (large size) based on the three species that he recognized. However, fenestrule length and width are not reflected on PCA-2 through PCA-5 (Table 9), which suggests that fenestrule size has not differentially affected the placement of *Cubifenestella* in the morphospace defined here. Small dissepiment and branch width, however, do play a role on PCA-4 (to the right on Figure 13.4, Table 9).

Laxifenestella. Morozova (1974) included moderately broad dissepiments in the original diagnosis of *Laxifenestella*. In addition to overall large features of PCA-1, dissepiment width is large on PCA-5 for *Laxifenestella* (to the bottom on Figure 13.1, Table 9). However, the *Laxifenestella* cloud is not differentiated on PCA-2 or PCA-4, which also contain dissepiment width as an important character. Therefore, breadth of dissepiments apparently has a negligible effect among the external characters of *Laxifenestella*.

Minilya. The original diagnosis of this genus included small nodes (Crockford 1944). The *Minilya* cloud is generally positive on PCA-3 (to the upper region on Figure 16.1, Table 9) but is roughly centered on both PCA–4 and PCA-5 (Figure 13.5). Node diameter may have had a small, but certainly not preeminent effect in determining the position of the *Minilya* cloud.

Spinofenestella. The original diagnosis of *Spinofenestella* Termier and Termier (1971)

Table 9. Genera represented by multiple species, with the position of each OTU cluster on each principal component axis and a list of the important characters for each axis (Table 4) and the magnitude (large or small observed values) for the measurements for the most diagnostic characters. For each PCA axis, OTUs that plot **HIGH** (positive values on scatter plots) represent specimens with some combination of characters that have *large measured values* for the characters with the most positive loading coefficients (Table 4, highlighted blue) and or *small measured values* for the characters with the most negative loading coefficients (Table 4, highlighted red). For each PCA axis, OTUs that plot **LOW** (negative values on scatter plots) represent specimens with some combination of characters that have *large measured values* for the characters with the most negative loading coefficients (Table 4, highlighted red) and or *small measured values* for the characters with the most positive loading coefficients (Table 4, highlighted blue).

Genus	Axis	Figure	Position	Measured values		
				Large	–	small
Alternifenestella						
	PCA-1	16.1	mixed		–	
	PCA-2	16.2	HIGH	**AAB**	–	AD, DW
	PCA-3	16.1-2	LOW	FL, NS, FW	–	**ND, AAB, AD**
	PCA-4	13.5	centered		–	
	PCA-5	13.5	HIGH	**AD, ALB**	–	DW, AAB, ND
Apertostella						
	PCA-1	14.5	mixed		–	
	PCA-2	14.6	LOW	DW, AD	–	**AAB**
	PCA-3	14.5-6	mixed		–	
	PCA-4	13.4	mostly centered		–	
	PCA-5	13.4	centered		–	
Archimedes					–	
	PCA-1	14.3	LOW		–	**all characters**
	PCA-2	14.4	LOW	DW, AD	–	**AAB**
	PCA-3	14.3-4	centered		–	
	PCA-4	13.3	centered		–	
	PCA-5	13.3	centered		–	
Cubifenestella					–	
	PCA-1	14.5	very HIGH	all characters	–	
	PCA-2	16.2	centered		–	
	PCA-3	16.1-2	centered		–	
	PCA-4	13.5	HIGH	AD, ND, NS	–	BW, DW
	PCA-5	13.5	centered		–	
Fenestella						
	PCA-1	11.5	LOW		–	**all characters**
	PCA-2	11.6	LOW	DW, AD	–	**AAB**
	PCA-3	11.5-6	centered		–	
	PCA-4	13.1	centered		–	
	PCA-5	13.1	centered		–	

Table 9 (continued).

Genus	Axis	Figure	Position	Measured values		
				Large	–	small
Hemitrypa						
	PCA-1	14.1	centered to LOW		–	**all characters**
	PCA-2	14.2	centered (low pca-3)		–	
			LOW (high pca-3)	DW, AD	–	**AAB**
	PCA-3	14.1-2	centered (mid pca-2)		–	
			HIGH (low pca-2)	AD, AAB, ND	–	FL, FW, NS
	PCA-4	13.2	mostly centered		–	
	PCA-5	13.2	mostly centered		–	
Laxifenestella						
	PCA-1	11.3	HIGH	**all characters**	–	
	PCA-2	11.4	centered		–	
	PCA-3	11.3-4	centered		–	
	PCA-4	13.1	centered		–	
	PCA-5	13.1	LOW	DW, AAB, ND	–	**AD, ALB**
Minilya						
	PCA-1	16.1	HIGH	**all characters**	–	
	PCA-2	16.2	HIGH	**AAB**	–	DW, AD
	PCA-3	16.1-2	HIGH	AD, AAB, ND	–	FL, FW, NS
	PCA-4	13.5	mixed		–	
	PCA-5	13.5	mixed		–	
Rectifenestella						
	PCA-1	11.1	LOW		–	**all characters**
	PCA-2	11.2	HIGH	**AAB**	–	DW, AD
	PCA-3	11.1-2	HIGH	AD, AAB, ND	–	FL, FW, NS
	PCA-4	13.1	centered		–	
	PCA-5	13.1	centered		–	
Spinofenestella						
	PCA-1	16.1	LOW		–	**all characters**
	PCA-2	16.2	HIGH	**AAB**	–	DW, AD
	PCA-3	16.1-2	LOW	FL, FW, NS	–	**AD, AAB, ND**
	PCA-4	6.5	centered		–	
	PCA-5	13.5	HIGH	AD, ALB	–	DW, AAB, ND

included short fenestrules. The *Spinofenestella* cloud is negative on PCA-3 (to the bottom on Figure 16.2, Table 9), which precludes especially short fenestrules.

In summary, for the five genera in which size of externally visible characteristics were mentioned when the genera were established, the mentioned characteristics have a small role (if any role at all) in determining placement of the genera in the nine-dimensional morphospace generated in this study.

Position Distribution of Each genus Within Defined Morphospace

Density and Size of Multispecies Coherent Clouds (PCA-1 vs. PCA-2 vs. PCA-3). Observations of *Rectifenestella* (seven nominal species), *Hemitrypa* (nine nominal species), *Archimedes* (five nominal species including the type species, *A. wortheni* Hall), *Cubifenestella* (three nominal species including the type species, *C. rudis* (Ulrich)), *Minilya* (two nominal species), and *Spinofenestella* (four nominal species) each formed their own single, coherent cloud.

The clouds of observations for each genus, while coherent, have varying size and density. The most observation-rich cloud, *Rectifenestella* (243), is dense and occupies a relatively small portion of morphospace located on the near zero negative portion of the PCA-1 axis (Figure 11.1-11.2). In contrast, the *Cubifenestella* cloud is represented by only 72 observations, which are very broadly distributed across the positive region of PCA-1 and equally broadly distributed though approximately centered on zero on both PCA-2 and PCA-3 (Figure 14.5-14.6).

The density and extent of the clouds for other multispecies coherent clouds (*Archimedes*, *Hemitrypa*, *Minilya,* and *Spinofenestella*) each fall between the end members. The cloud of OTUs for *Archimedes* largely overlaps that of *Fenestella* (Figures 14.3-14.4 and 13.3). The cloud of OTUs for *Hemitrypa* is similar to that of *Rectifenestella* (Figures 14.1-14.2 and 13.1-13.2), however, the *Hemitrypa* cloud has an asymmetrical distribution as the overall size of characters become larger. That is, larger PCA-1 values of *Hemitrypa* (toward the right on PCA-1, Figure 14.1) expand into the positive region of PCA-3 and into the negative region of PCA-2 (upper left quadrant, Figure 14.2). *Hemitrypa* is one of the few examples among the genera analyzed that does not correspond to a single geometric shape such as a conical cloud or truncated ellipsoid, i.e., apparently at least two

somewhat independent controls affect the distribution of *Hemitrypa* OTUs in this morphospace.

The OTUs for *Minilya* represent only two nominal species, but they form a coherent cloud, expanding into larger values for PCA-3 and PCA-2 with larger overall size (Figure 16.1-16.2). Additional specimens and/or species of *Minilya* would provide an excellent test to establish whether morphospace would be filled for the existing distribution or whether the cloud would expand (toward more negative PCA-3) to mimic the conical shape of the clouds of several other genera or confirm an elongated cloud.

The cloud of OTUs for *Spinofenestella* (and *Alternifenestella* in part) overlaps parts of the clouds for *Fenestella* and *Archimedes*, but forms a much smaller cloud, largely restricted to negative PCA-3 values and centered on more positive values for PCA-2 (c.f. Figures 16.1-16.2 and 14.1-14.4).

Regardless of the density of packing of observations for these genera represented by two or more species, each occupies a well-delimited portion of the morphospace that partially overlaps the morphospace of other genera but which has its own unique pattern and centroid. In other words, these genera have morphologies that can be used to discriminate them more or less confidently from at least a subset of the other genera. Although they were defined exclusively or largely on characteristics other than size, they also can be described by a separate set of external, size-determined characteristics.

Multispecies Discontinuous Clouds. Observations of *Laxifenestella* (six nominal species), *Fenestella* (five nominal species), *Apertostella* (three nominal species including the type species *A. crassata* Snyder 1991), and *Alternifenestella* (five nominal species) are organized into two separate clouds for each of the genera. In each case one of the clouds is formed by a single nominal species, and all the other nominal species (ranging from two to five) comprise the other cloud. There are three possible reasons for the discontinuity in distribution of observations assigned to a single genus: 1) there are other species within the genus that if included in the study would have bridged the gap, 2) size characteristics of a species are not phylogenetically constrained and do not necessarily form a continuum, and 3) the single isolated species was incorrectly assigned in the study from which the data were taken for the present study.

The isolated species in *Laxifenestella* was originally named *Fenestella serratula* Ulrich, 1890,

reassigned to *Laxifenestella,* and measured in Snyder (1991). *F. serratula* has strong morphological affinity with *Laxifenestella sarytshevae* (Shul'ga-Nesterenko 1951), the type species of *Laxifenestella*, having all the qualitative characters included in the original generic diagnosis given by Morozova (1974) and visible in the type specimens of *F. sarytshevae* (illustrated in Morozova 2001). Other than the isolated position in morphospace, there is no apparent reason to question determination of *F. serratula* as a species of *Laxifenestella*. Excluding the discrete subcluster noted above, the majority of *Laxifenestella* observations form a truncated ellipsoid (positive of 0.0 on PCA-1) near a boundary with *Rectifenestella* (Figure 11.3), reflecting an overall larger size for measured characters.

A large cloud, comprised of observations derived from four *Fenestella* species is elongated on PCA-3, centered on PCA-1, and located on the negative portion of the PCA-2 axis (Figure 11.5-11.6). *Fenestella* sp. 1 of Ernst and Schroeder (2007) plots separately, forming an isolated, small cloud between -1.0 and -2.0 on PCA-1 (Figure 11.5).

Fenestella sp. 1 (Ernst and Schroeder 2007) appears to have greater affinity with *Rectifenestella* than with *Fenestella s.s*. It has elongate pentagonal zooecial chamber cross-sectional shape in the endozone and moderately large keel nodes (Ernst and Schroeder 2007, p. 218, figure 6E-H), which are characteristic of *Rectifenestella* but different from the slightly elongate rectangular zooecial cross-sectional chamber shape in the endozone and small or absent keel nodes characteristic of *Fenestella subantiqua* (d'Orbigny 1850), the type species of *Fenestella*, as described by Snell (2004). If *Fenestella* sp. 1 (Ernst and Schroeder 2007) were reassigned to *Rectifenestella* on the basis of its zooecial chamber shape and the presence of conspicuous nodes, it would form a contiguous part of the *Rectifenestella* observations on PCA-1, PCA-2, and PCA-3 (Figure 11.5-11.6).

Apertostella forms two disjoint but independently coherent clouds. One subcluster consists of two species, including the type species, *A. crassata* Snyder, 1991. This subcluster occupies morphospace shared by *Fenestella* (PCA-1 values from -1.0 to +1.0 and PCA-3 values from -1.0 to +1.5) and is restricted to negative values on PCA-2 (Figures 14.5-14.6). This group of observations bridges the gap on PCA-1 between *Rectifenestella* and *Cubifenestella* (Figure 14.5), is centered on PCA-3, and is centered farther left on PCA-2 than

either *Rectifenestella* or *Cubifenestella* (Figure 14.6).

The second subcluster of *Apertostella*, composed solely of the species *Apertostella venusta* Snyder, 1991, occupies morphospace independent of any other genus in this study. It is adjacent to *Cubifenestella*, overlapping it but extending even farther into positive values on PCA-1 (Figure 14.5). However, it has more negative PCA-3 values than the *Cubifenestella* observations that it overlaps on PCA-1.

Morozova (2001) considered *Cubifenestella* and *Apertostella* to be synonyms of *Rectifenestella*. She argued that the proportions of length:width:height ratios of endozonal chambers that Snyder used in part to characterize the genera were encompassed in the concept of *Rectifenestella*. She also mistakenly interpreted a small, strategically placed and oriented dog-tooth crystal of calcite as a superior hemiseptum in an illustration (Snyder 1991, Pl. 30, figure 5) of the type species of *Cubifenestella*; superior hemisepta are characteristic for *Rectifenestella* but according to Snyder (1991) are absent in *Cubifenestella* and *Apertostella*. The distribution of observations of the three putative genera on PCA-1, PCA-2, and PCA-3 do form a continuum. One subcluster of *Apertostella*, comprised in part by its type species, bridges the gap between *Rectifenestella* and *Cubifenestella*, and the other subcluster of *Apertostella*, together with the *Cubifenestella* observations, extends the cone formed in negative PCA-1 space well into positive PCA-1 space and expands it in PCA-2 and PCA-3 space (Figure 14.5-14.6).

The distributions in morphospace represented in Figure 14.5-14.6 suggest a closer affinity of *Apertostella venusta* with species that comprise *Cubifenestella* than with the other two species originally included in *Apertostella*. If the absence of a superior hemiseptum is considered sufficient to exclude the subcluster of *Apertostella* observations centered at the crossing of the PCA-1 and PCA-3 axes from *Rectifenestella*, then the two species that comprise that subcluster need to be closely examined to determine if they warrant discrimination from *Cubifenestella*. The discrimination of these three genera from one another requires further study.

Alternifenestella observations group into two subclusters, one of which is comprised of observations from four species and corresponds with the placement of *Spinofenestella*, i.e., slightly negative on PCA-1 and PCA-3, and slightly positive on PCA-2 (Figure 16.1-16.2).
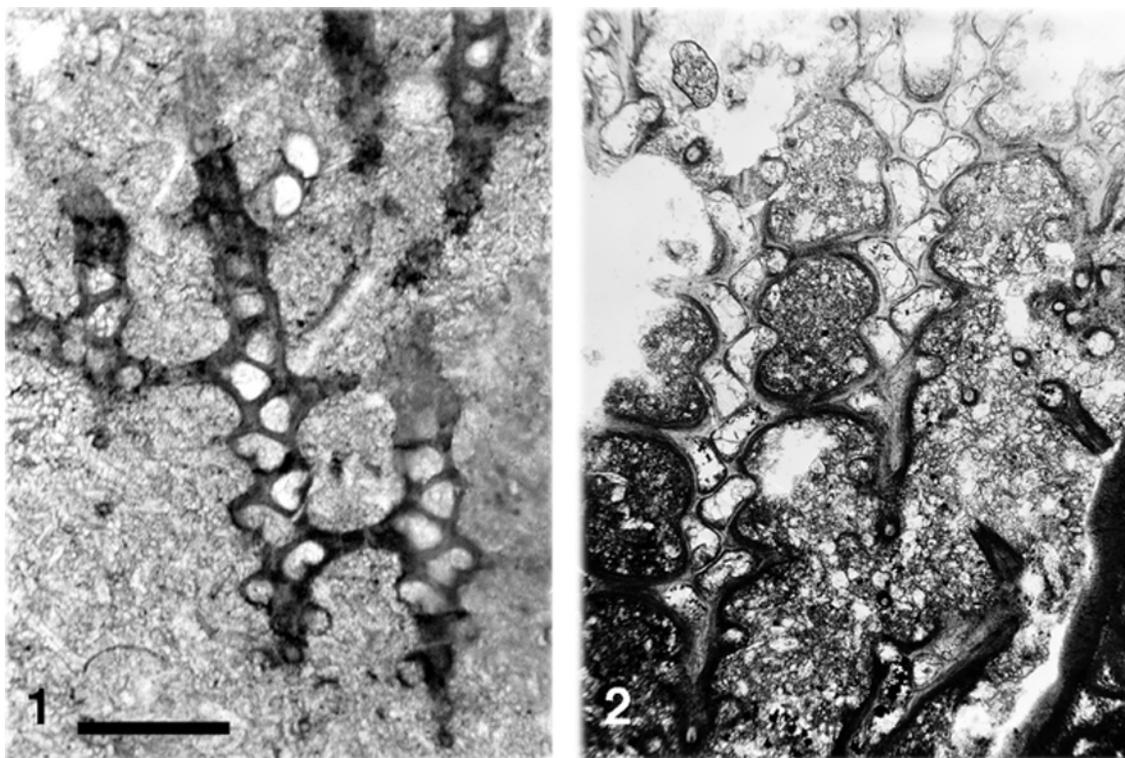
FIGURE 17. Original type specimens of type species of *Alternifenestella* and *Spinofenestella*. (1) tangential section of *Fenestella donaica* (Lebedev) var. *minor* Nikiforova, 1933b (Middle Carboniferous, Bashkirian, Donets Basin, Ukraine), Paleontological Institute Moscow PIN 15/60a/33, type species of *Alternifenestella*; (2) tangential section of *Fenestella spinulosa* Condra, 1902 (Burr Limestone?, Lower Permian, Nebraska, USA), University of Nebraska paleontology collection 133311, type species of *Spinofenestella*. Scale bar equals 500 μm in Figure 17.1 for both photographs.

The original diagnoses of *Alternifenestella* and *Spinofenestella* included two similarities (presence of a keel, single row of keel nodes). Termier and Termier (1971) indicated regular, short fenestrules and occurrence of an aperture at the base of each dissepiment for *Spinofenestella*, features not mentioned in Morozovas characterization of the genus three years later (1974). The only differences that Morozova (1974) indicated for the two genera were branch width (wide in *Spinofenestella*, thin in *Alternifenestella*) and basal shape of endozonal zooecial chambers (triangular in *Spinofenestella*, triangular-trapeziform in *Alternifenestella*). The co-occurrence of *Spinofenestella* and the second subcluster of *Alternifenestella* in morphospace as defined by PCA-1, PCA-2, and PCA-3 invite reevaluation of these genera.

Comparison of original type specimens of *Alternifenestella* and *Spinofenestella* reveals no differences in qualitative characters and even minimal differences in quantitative characteristics (Figure 17). In type specimens of both species, branch width is essentially equal and zooecial cross-sec-

tional shape in deep tangential sections is triangular. The apparent foreshortening of endozonal chambers of *Fenestella donaica minor* (Figure 17.1) relative to those of *F. spinulosa* (Figure 17.2) is due at least in part to the greater distal downward inclination of the thin section of *F. donaica minor* relative to that of *F. spinulosa*. The contention by Morozova (1974) that branches are relatively broader in *Spinofenestella* and that deep cross sections of zooecial chambers of *Alternifenestella* encompass trapezoidal shapes lacking in *Spinofenestella* must have been based on other species included in her concept of the two genera.

Based on such close correspondence in morphology as seen in thin sections of the type species, supported by correspondence of externally determined morphospace (Figure 16.1-16.2) as expressed in several non-type species assigned to the two genera analyzed in the current study, we consider *Alternifenestella* and *Spinofenestella* to be subjective synonyms. Termier and Termier (1971, p. 42) named both genera on the same

page. There is no objective criterion for determining that one of the genera should have priority over the other, but we prefer to give *Spinofenestella* priority because although both genera were given a legal basis for naming (i.e., designation of a type species) only *Spinofenestella* was provided with a diagnosis by Termier and Termier (1971).

The second subcluster comprised of *A. bifida* (Eichwald 1860) in Nakrem (1994) is positive on PCA-1 and extends into the positive region of PCA-3 (Figure16.1). These observations are from a single specimen assigned to *Alternifenestella bifida* (Eichwald) in Nakrem (1994). The positive distribution of this subcluster of *Alternifenestella* indicates overall large sizes, with a positive range on PCA-1 (Figure 16.1) similar to that of *Minilya*, which is characterized by a double row of keel nodes. Observations of *bifida* are scattered but centered on PCA-3, and their slightly positive placement on PCA-2 indicates some combination of small apertures, narrow dissepiments, and/or distantly spaced apertures along branches. Nakrem's specimen has a single row of keel nodes, and zooecial chambers have triangular cross sections in deep tangential sections. Despite its more robust features (Figure 16.1) as measured externally, it therefore appears to belong within the generic concept *Spinofenestella* based on chamber shape and the single row of keel nodes rather than to *Minilya*.

Genera Represented by Single Species. The central position of observations in the single species of *Exfenestella* and *Wjatkella* (centroids of their respective clouds plotting near zero on PCA-1, PCA-2, and PCA-3; Figure 16.316.4, Table 10) gives no indication of distinctive size of their exterior features. Although additional species would undoubtedly give some idea of whether these species trend out into some oriented direction within the morphospace, the position of the two species indicates that at least their respective genera include species that have no distinctive size characteristics of any kind. In contrast, the distinctly positive PCA-1 position of observations from the single species of *Flexifenestella* (Figure 16.3) indicates overall large size, and their negative position on PCA-3 (Figure 16.3-16.4) is notable. Whatever other characters may be involved in the negative placement on PCA-3, the negative PCA-3 loading of large fenestrules is sure to be involved, because the species included here and *Flexifenestella* overall is characterized by broad branches that are highly sinuous (Morozova 1974), the sinuosity generating unusually large fenestrules for a fenestellid taxon.

Two species in the study are not biserial fenestellids and were intended to serve as reference points. One, *Lyroporella*, has branches organized like those of *Polyporella*, with two rows of zooecia distal to bifurcations but proliferating to three rows at an appreciable distance preceding the next bifurcation. The second, *Anastomopora anaphora*, typically has multiserial branches but in some species – such as the one included here – branch segments begin with only two rows of zooecia after a bifurcation before interpolating additional rows of zooecia. Even though having large sections of branches with sufficient width to accommodate three rows of zooecia rather than two, *Lyroporella* surprisingly is characterized overall by small exterior measurements, occurring near the edge of the composite cloud on the *negative* end of PCA-1 (Figure 14.1). The slightly positive position on PCA-3 (Figure 14.1-14.2) and slightly negative position on PCA-2 (Figure 14.2) are almost certainly strongly influenced by small fenestrules and wide dissepiments. Lyre shaped bryozoans in general tend to have closely spaced branches and broad dissepiments, resulting in small fenestrules that comprise an anomalously small (15%) proportion of the fenestrate sheet (McKinney et al. 1993). These structural features, which apparently are related to the overall colony morphology and its relation to the highly kinetic environment in which the colonies lived (McKinney 1977) may be largely responsible for the location of the *Lyroporella* cloud within the densely packed conical (negative PCA-1) end of the composite cloud.

The second control, *Anastomopora anaphora,* would be predicted to plot anomalously high on PCA-1, because the species typically has three to four rows of zooecia along branches (McColloch et al. 1994), which would be predicted to require greater branch width than fenestellids with two rows. Polyporid fenestrates with three to four rows of zooecia typically have larger branch widths and disproportionately larger branch spacing (i.e., relatively wider fenestrules) than do fenestellids (Starcher and McGhee 2002). Indeed, *Anastomopora's* positive position on PCA-1 (Figure 14.3) reflects larger overall sizes, but it falls well below the high end of the PCA-1 range of *Laxifenestella* (Figure 11.3), *Cubifenestella* (Figure 14.5), *Apertostella* (Figure 14.5), and *Minilya* (16.1). *Anastomopora* observations are almost centered on zero for PCA-3, but on PCA-2 they extend from the center of the composite cloud of all fenestellid observations to include the highest negative value in the study (Figure 16.4), minimally beyond the most

Table 10. Genera represented by single species, with the position of each OTU cluster on each principal component axis and a list of the important characters for each axis (Table 4) and the magnitude (large or small observed values) for the measurements for the most diagnostic characters. See Table 9 for additional explanation of the labeling and interpretation.

Genus	Axis	Figure	Position	Large	–	small
					Measured values	
Anastomopora						
	PCA-1	16.3	very HIGH	all characters	–	
	PCA-2	16.4	very LOW	DW, AD	–	**AAB**
	PCA-3	16.3-4	LOW	FL, FW, NS	–	**AD, AAB, ND**
	PCA-4	13.6	very LOW	DW, BW	–	**ND, NS, AD**
	PCA-5	13.6	centered		–	
Exfenestella						
	PCA-1	16.3	slightly HIGH	all characters	–	
	PCA-2	16.4	HIGH	AAB	–	DW, AD
	PCA-3	16.3-4	slightly HIGH	AD, AAB, ND	–	FL, FW, NS
	PCA-4	13.6	slightly HIGH	AD, ND, NS	–	BW, DW
	PCA-5	13.6	slightly LOW	FL, FW, NS	–	**AD, AAB, ND**
Flexifenestella						
	PCA-1	16.3	very HIGH	all characters	–	
	PCA-2	16.4	slightly HIGH	AAB	–	DW, AD
	PCA-3	16.3-4	LOW	FL, FW, NS	–	**AD, AAB, ND**
	PCA-4	13.6	slightly LOW	DW, BW	–	ND, NS, AD
	PCA-5	13.6	HIGH	AD, ALB	–	DW, AAB, ND
Lyroporella						
	PCA-1	14.1	very LOW		–	**all characters**
	PCA-2	14.2	very LOW	DW, AD	–	**AAB**
	PCA-3	14.1-2	HIGH	AD, AAB, ND	–	FL, FW, NS
	PCA-4	13.2	HIGH	AD, ND, NS	–	BW, DW
	PCA-5	13.2	LOW	FL, FW, NS	–	**AD, AAB, ND**
Wjatkella						
	PCA-1	16.5	LOW		–	**all characters**
	PCA-2	16.6	LOW	DW, AD	–	**AAB**
	PCA-3	16.5-6	HIGH	AD, AAB, ND	–	FL, FW, NS
	PCA-4	13.6	very LOW	DW, BW	–	**ND, NS, AD**
	PCA-5	13.6	HIGH	AD, ALB	–	**DW, AAB, ND**

negative values for *Laxifenestella* (Figure 11.4) and *Apertostella* (Figure 14.6). Negative values for PCA-2 are due to some combination of large apertures, wide dissepiments, and close spacing of apertures along branches (Figure 4), more than to large branch width and large fenestrules.

Lyroporella and *Anastomopora* are currently assigned to two separate families differentiated from the Fenestellidae, thus they have appreciable

morphological differences from each other and the rest of the genera included. Nevertheless, they plot within the borders of the composite cloud of fenestellid observations. Their inclusion within this morphospace supports the interpretation that the multispecies fenestellid genera represent appreciable differences in gross morphology among genera.

Relationships Among Morphometric Characters

It is not surprising that a strong degree of covariance exists among morphometric characters (Table 8). However, the combination of characters and their relative significance is noteworthy.

These relationships among covarying characters and relationships expressed in PCA loading coefficients (Table 4) invite interpretation of their biological significance, if any. However, the relationships are complex and in places contradictory among methods of analysis. Future work in this area will require partitioning of parameters of both size and shape.

1. The first complex (FL-FW-ALB-NS) involves a relationship between fenestrule size and spacing of apertures laterally across branch (but not so much along branch) (Table 8, red highlight). Fenestrule size (meshwork openness vs. compactness) is typically associated with water currents and feeding. Characters of aperture spacing are associated with lophophore and polypide size. Thus, the inclusion of node spacing in this character complex is somewat puzzling.

2. The second complex of covaring characters (AAB-ALB-ND) involves spacing of apertures (both along and lateral to branch) and node diameter. Again, features of apertural spacing are typically associated with lophophore and polypide size, which makes the inclusion of node spacing in this character complex enigmatic (Table 8, purple).

3. The third complex of covaring characters (BW-DW) is associated with the robustness of the meshwork (branch and dissepiment width) (Table 8, blue).

4. The fourth complex of covaring characters (AD-ND) is associated with the size of both apertures and nodes (Table 8, green). The biological significance of this relationship is unclear.

5. The combination of aperture size and the spacing of apertures along branch (AD-AAB)

displays the least (though still marginally significant at p = 0.02) covariance of all character pairs (Table 8, orange). This weak relationship may reflect an independent relationship between lophophore diameter and length of space required to accommodate polypides when retracted, perhaps reflecting independence of lophophore size and whether or not the polypide is doubled onto itself or does or does not include tentacle wrinkling when retracted.

SUMMARY

The localized distribution in morphospace of groups of species assigned to some of the genera established by subdivision of *Fenestella s.l.* lends weight to the recognition of the recently named genera as morphological characterizable groups. This coherent clustering does not demonstrate that the genera as currently recognized are phylogenetically determined entities but instead adds a new dimension to the argument that they are morphologically coherent, which is consistent with the hypothesis that they are distinct clades. Where data from species assigned to one of the genera are organized into two distinct clouds, an opportunity is provided to evaluate the reason for the gap, which involves the possibilities that inclusion of additional species in the genus would have closed the gap, that one or more species has been misassigned to genus and belongs to a different named genus, or that one of the disjoint sections of the cloud may represent an as yet unnamed genus. In addition, correspondence in the morphospace of genera with subtle putative differences (such as for *Spinofenestella* and *Alternifenestella*), invites reconsideration of whether or not the two are indeed different or should be considered as a single genus.

Although the methodology of evaluating a priori generic assignments based largely on characters other than the ones used in original diagnoses provides insights, we do not advocate that exterior characters from this study be used alone as criteria for the recognition of biserial fenestellid Bryozoa genera.

ACKNOWLEDGMENTS

and the University Research Council of Appalachian State University.

REFERENCES

Bassler, R.S. 1953. Bryozoa, p. G1-G253. In Moore, R.C. (ed.), *Treatise on Invertebrate Paleontology, Part G, Bryozoa.* Geological Society of America and University of Kansas Press, Boulder, Colorado, and Lawrence, Kansas, 1-253.

Busk, G. 1884. Report on the Polyzoa – The Cheilostomata. *Report on the Scientific Results of the Voyage of HMS Challenger during the years 1873-76. Zoology. volume 10, part 30.* Her Majestys Stationary Office, London.

Condra, G.E. 1902. New Bryozoa from the Coal Measures of Nebraska. *American Geologist,* 30:337-359.

Crockford, J. 1944. Bryozoa from the Wandagee and Nooncabah Series (Permian) of Western Australia*. Journal of the Royal Society of Western Australia*, 28:165-185.

d'Orbigny, A. 1850. *Prodrome de paléontologie stratigraphique universelle des animaux mollusques & rayonnés. Volume 1.* Victor Masson, Paris.

Eichwald, E. d' 1860. *Lethaea rossica ou Paléontologie de la Russie,* 1. E. Scheizerbart: Stuttgart, Germany. 681 pp.

Ernst, A. 2001. Bryozoa of the Upper Permian Zechstein Formation of Germany. *Senckenbergiana Lethaea*, 81:135-181.

Ernst, A. and Schroeder, A. 2007. Stenolaemate bryozoans from the Middle Devonian of Rhenish Slate Massif (Eifel, Germany). Neues Jahrbuch für Geologie und Paläontologie - Abhandlungen, 246:205-233.

Ernst, A. and Winkler-Prins, C.F. 2008. Pennsylvanian bryozoans from the Cantabrian Mountains (northwestern Spain). *Scripta Geologica*, 137:1-123.

Ernst, A., Senowbari-Daryan, B., and Koorosch, R. 2008. Permian Bryozoa from the Jamal Formation of Shotori Mountains (northeast Iran). *Revue de Paléobiologie, Genève*, 27:395-408.

Hageman, S.J. 1991. Discrete morphotaxa from a Mississippian fenestrate faunule: presence and implications, p. 147-150. In Bigey, F.P. (ed.), *Bryozooaries actuel et fossile: Bryozoans living and fossil. Bulletin de la Société des Sciences Naturelles de l'Ouest de la France*, Mémoire HS 1.

Hageman, S.J. 1992. Alternative methods for dealing with non-normality and heteroscedasticity in paleontologic data. *Journal of Paleontology*, 66:857-867.

Hageman, S.J., Needham, L.L., and Todd, C.D. 2009. Threshold effects of food concentration on the skeletal morphology of the bryozoan *Electra pilosa* (Linnaeus, 1767). *Lethaia*, published Online 25 Mar 2009.

Hall, J. 1857. Observations on the genus *Archimedes*, or *Fenestella*, with descriptions of species, etc. *Proceedings of the American Association for the Advancement of Science*, 10:176-180.

Hammer, Ø., Harper, D.A.T., and Ryan, P.D. 2001. PAST: Palaeontological statistics software package for education and data analysis. *Palaeontolgia Electronica* Vol. 4, Issue 1; 9p, 178KB; http://palaeo-electronica.org/2001_1/past/issue1_01.htm

Holdener, E.J. 1994. Numerical taxonomy of fenestrate bryozoans: Evaluation of methodologies and recognition of intraspecific variation. *Journal of Paleontology*, 68:1201-1214.

Lebedev, N. 1924. Materialiy dlya geologii Donetskogo kamennougol'nogo bassena. *Izvestiya Ekaterinoslavskogo Gornogo Instituta, ser. 2*, 14:1-114.

Lonsdale, W. 1839. Corals, p. 675-694. In Murchison, R.I. (ed.), *The Silurian System, founded on geological researches in the counties of Salop, Hereford, Radnor, Montgomery, Caermarthen, Brecon, Pembroke, Monmouth, Gloucester, Worcester, and Stafford; with Descriptions of the Coal-fields and Overlying Formations*. John Murray, London.

McColloch, M.E., Gilmour, E.H., and Snyder, E.M. 1994. The Order Fenestrata (Bryozoa) of the Toroweap Formation (Permian), southern Nevada. *Journal of Paleontology*, 68:746-762.

McKinney, F.K. 1977. Functional interpretation of lyre-shaped Bryozoa. *Paleobiology*, 3:90-97.

McKinney, F.K. 1994. The bryozoan genera *Lyropora* and *Lyroporidra* (Order Fenestrida, Family Polyporidae) in Upper Mississippian (Chesterian) rocks of eastern North America. *American Museum Novitates*, 3111:1-31.

McKinney, F.K. and Jackson, J.B.C. 1991. *Bryozoan Evolution.* The University of Chicago Press, Chicago.

McKinney, F.K. and Kriz, J. 1986. Lower Devonian Fenestrata (Bryozoa) of the Barrandian area, Prague Basin, Bohemia, Czechoslovakia. *Fieldiana Geology (n. s.)*, 15:1-90.

McKinney, F.K., Taylor, P.D., and Zullo, V.A. 1993. Lyre-shaped hornerid bryozoan colonies: homeomorphy in colony form between Paleozoic Fenestrata and Cenozoic Cyclostomata. *Journal of Paleontology*, 67:343-354.

Miller, S.A. 1889. *North American Geology and Palaeontology.* Western Methodist Book Concern, Cincinnati, Ohio.

Morozova, I.P. 1970. Mshanki pozdnei permi. *Akademiya Nauk SSSR Trudy Paleontologicheskogo Instituta*, 122:1-347.

Morozova, I.P. 1974. Reviziya roda *Fenestella. Paleontologicheskiy Zhurnal*, 1974 (2):54-67.

Morozova, I.P. 2001. Mshanki otryada Fenestellida. *Trudy Paleontologicheskogo Instituta*, 277:1-176.

Muir-Wood, H. and Cooper, G.A. 1960. Morphology, classification and life habits of the Productoidea (Brachiopoda). *Geological Society of America Memoir*, 81:1-447.

Nakrem, H.A. 1994. Middle Carboniferous to Early Permian bryozoans from Spitsbergen. *Acta Paleontologica Polonica*, 39:45-116.

Nakrem, H.A. 1995. Bryozoans from the Lower Permian Voringen Member (Kapp Starostin Formation), Spitsbergen, Svalbard. *Norsk Polarinstitutt Skrifter*, 196:1-93.

Nekhoroshev, V.P. 1926. Altayskie Reteporinae tarkhanskoy svity. *Izvestiya Geologicheskogo Komiteta*, 44:785-803.

Nekhoroshev, V.P. 1928. Istoriya razvitiya paleozoyskikh mshanok semeystva Fenestellidae. *Izvestiy Geologicheskogo Komiteta*, 47:479-518.

Nekhoroshev, V.P. 1932. Mikroskopicheskiy metod issledovaniya paleozoiskikh mshanok sem. Fenestellidae. *Izvestiya Vsesoiuznogo Geologo-Razvedochnogo Ob"edineniya*, 51:279-303.

Nekhoroshev, V.P. 1979. O neratsionalnosti razdeleniya roda *Fenestella*. *Ezhegodnik Vsesoyuznogo Paleontologicheskogo Obshchestva*, 22:287-294.

Nickles, J.M. and Bassler, R.S. 1900. A synopsis of American fossil Bryozoa, including bibliography and synonomy. United States Geological Survey Bulletin 173.

Nikiforova, A.I. 1933a. Kamennougolnye otlozheniya stredne Azii. *Trudy Vsesoyuznogo Geologo-Razvedochnogo Ob"edineniya NKTP SSSR*, 207:1-78.

Nikiforova, A.I. 1933b. Sredne-kamennougol'nye mshanki Donetskogo bassena [Middle Carboniferous Bryozoa of the Donets Basin]. Trudy Vsesoiuznogo Geologo-Razvedochnogo Ob"edineniia NKTP SSSR [Transactions of the United Geological and Prospecting Service of USSR] 237:1-46.

Nikiforova, A.I. 1933c. Verkhne-paleozoskie mshanki Dzhulfinskogo raona. *Trudy Vsesoyuznogo Geologo-Razvedochnogo Ob"edineniya NKTP* SSSR, 364:1-44.

Nikiforova, A.I. 1938. Tipy kamennougol'nykh mshanok europeyskoy chasti SSSR. *Paleontologiya SSSR*, 4 (pt. 5, fasc. 1):1-290.

Owen, D.D. 1838. *Report of a geological reconnoisance [sic] of the State of Indiana; made in the year 1837*. Bolton & Livingston, Indianapolis, Indiana.

Phillips, J. 1841. *Figures and Descriptions of the Palaeozoic Fossils of Cornwall, Devon, and West Somerset; Observed in the Course of the Ordnance Geological Survey of that District*. Longman, Brown, Green, & Longmans, London.

Rohlf, F.J. and Sokal, R.R. 1981. *Statistical Tables* (second edition). W.H. Freeman and Company, New York.

Shulga-Nesterenko, M.I. 1941. Nizhnepermskie mshanki Urala. *Paleontologiya SSSR*, 5 (pt. 5, fasc. 1):1-276.

Shul'ga-Nesterenko, M.I. 1951. Carboniferous fenestellids of the Russian Platform. *Trudy Paleontologicheskogo Instituta Adademiia Nauk SSSR*, 32:1-161.

Simpson, G.B. 1895. A discussion of the different genera of Fenestellidae, p. 687-727. In *Thirteenth Annual Report of the State Geologist* [of New York] *for the year 1893*. Albany.

Simpson, G.B. 1897. A handbook of the genera of the North American Palaeozoic Bryozoa, p. 407-669. In *Fourteenth Annual Report of the State Geologist* [of New York] *for the year 1894*. Albany.

Snell, J. 2004. Bryozoa from the Much Wenlock Limestone (Silurian) formation of the West Midlands and Welsh Borderland. *Palaeontographical Society Monograph*, 157(621):1-110.

Snyder, E.M. 1991. Revised taxonomic procedures and paleoecological applications for some North American Mississippian Fenestellidae and Polyporidae (Bryozoa). *Paleontographica Americana*, 57:1-275.

Snyder, E.M. and Gilmour, E.H. 2006. New fenestrate Bryozoa of the Gerster Limestone (Permian) Medicine Range, Northeastern Nevada. *Journal of Paleontology*, 80:867-888.

Starcher, R.W. and McGhee, G.R. Jr. 2002. Theoretical morphology of modular organisms: geometric constraints of branch and dissepiment width and spacing in fenestrate bryozoans. *Neues Jahrbuch für Geologie und Paläontologie Abhandlungen*, 223:79-122.

Termier, H. and Termier, G. 1971. Bryozoaires du paleozoique superieur de l'Afghanistan. *Documents des Laboratoires de Géologie de la Faculté des Sciences de Lyon*, 47:1-52.

Ulrich, E.O. 1890. Palaeozoic Bryozoa. *Illinois Geological Survey,* 8:283-688.

Winston, J.E. 1977. Feeding in marine bryozoans, p. 233-271. In Woollacott, R.M. and Zimmer, R.L. (eds.), *The Biology of Bryozoans*. Academic Press, New York.

Winston, J.E. 1978. Polypide morphology and feeding behavior in marine ectoprocts. *Bulletin of Marine Science,* 28:1-31.

APPENDIX

Genus and Species	Number of Composite OTUs	Geologic Period	Geographic Location	Data Type	Source	Number of Colonies
Alternifenestella	(50 total)					
A. bifida	12	Permian	Spitsbergen	reconstructed	Nakrem, 1995	1
A. estrelita	2	Devonian	Czech Republic	measured	McKinney, unpub.	2
A. sp. 1	12	Devonian	Germany	reconstructed	Ernst & Schroeder, 2007	1
A. sp. 2	12	Devonian	Germany	reconstructed	Ernst & Schroeder, 2007	4
A. cf. *tenuiseptata*	12	Permian	Spitsbergen	reconstructed	Nakrem, 1995	3
Anastomopora	(12 total)					
*A. anaphora**	12	Permian	Nevada	reconstructed	McColloch et al., 1994	?
Apertostella	(60 total)					
A. foramenmajor	24	Mississippian	Illinois Basin	measured	Snyder, 1991	3 to 12
A. crassata	24	Mississippian	Illinois Basin	measured	Snyder, 1991	3 to 6
A. venusta	12	Mississippian	Illinois Basin	measured	Snyder, 1991	3 to 6
Archimedes	(60 total)					3 to 6
A. negligens	12	Mississippian	Illinois Basin	reconstructed	Snyder, 1991	3 to 6
A. owenanus	12	Mississippian	Illinois Basin	measured	Snyder, 1991	3 to 6
A. sp. B	12	Permian	Spitsbergen	reconstructed	Nakrem, 1994	2
A. valmeyeri	12	Mississippian	Illinois Basin	measured	Snyder, 1991	3 to 6
A. worktheni	12	Mississippian	Illinois Basin	measured	Snyder, 1991	3 to 6
Cubifenestella	(72 total)					
C. globodensata	24	Mississippian	Illinois Basin	measured	Snyder, 1991	3 to 12
C. rudis	24	Mississippian	Illinois Basin	measured	Snyder, 1991	3 to 12
C. usitata	24	Mississippian	Illinois Basin	measured	Snyder, 1991	3 to 12
Exfenestella	(24 total)					
E. exigua	24	Mississippian	Illinois Basin	measured	Snyder, 1991	3 to 12
Fenestella	(60 total)					
F. akselensis	12	Permian	Spitsbergen	reconstructed	Nakrem, 1995	6
F. reversicnotta	12	Permian	Spitsbergen	reconstructed	Nakrem, 1995	7
F. sp. 1	12	Devonian	Germany	reconstructed	Ernst & Schroeder, 2007	3
F. sp. 2	12	Devonian	Germany	reconstructed	Ernst & Schroeder, 2007	2
F. sp. 3	12	Devonian	Germany	reconstructed	Ernst & Schroeder, 2007	2
Flexifenestella						
F. cf. *grandis*	12	Permian	Spitsbergen	reconstructed	Nakrem, 1994	1
Hemitrypa	(225 total)					
H. aprilae	12	Mississippian	Illinois Basin	measured	Snyder, 1991	3 to 6
H. aspera	12	Mississippian	Illinois Basin	reconstructed	Snyder, 1991	3 to 6
H. bohemicus	12	Devonian	Czech Republic	measured	McKinney, unpub.	3
H. hemitrypa	12	Mississippian	Illinois Basin	reconstructed	Snyder, 1991	3 to 6
H. linotheras	21	Devonian	Czech Republic	measured	McKinney, unpub.	4
H. mimicra	41	Devonian	Czech Republic	measured	McKinney, unpub.	6
H. perstriata	12	Mississippian	Illinois Basin	reconstructed	Snyder, 1991	3 to 6
H. tenella	79	Devonian	Czech Republic	measured	McKinney, unpub.	9
H. vermifera	24	Mississippian	Illinois Basin	measured	Snyder, 1991	3 to 6
Laxifenestella	(117 total)					
L. capilosa	15	Devonian	Czech Republic	measured	McKinney, unpub.	3
L. coniunctistyla	24	Mississippian	Illinois Basin	measured	Snyder, 1991	3 to 12
L. digittata	5	Devonian	Czech Republic	measured	McKinney, unpub.	1
L. maculasimilis	24	Mississippian	Illinois Basin	measured	Snyder, 1991	3 to 12
L. serratula	24	Mississippian	Illinois Basin	measured	Snyder, 1991	3 to 12
L. fluctuata	24	Mississippian	Illinois Basin	measured	Snyder, 1991	3 to 12
Lyroporella	(12 total)					
*L. serissima**	12	Permian	Spitsbergen	reconstructed	Nakrem, 1995	4
Minilya	(48 total)					
M. sivonella	24	Mississippian	Illinois Basin	measured	Snyder, 1991	3 to 12
M. paratriserialis	24	Mississippian	Illinois Basin	measured	Snyder, 1991	3 to 12
Rectifenestella	(273 total)					
R. exilis	6	Devonian	Czech Republic	measured	McKinney, unpub.	1
R. limbata	147	Pennsylvanian	Kansas	measured	Holdener 1994	21
R. microporata	24	Permian	Spitsbergen	reconstructed	Nakrem, 1994 & 1995	3 (1994)
R. multispinosa	24	Mississippian	Illinois Basin	measured	Snyder, 1991	3 to 12

R. retiformis	24	Permian	Spitsbergen	reconstructed	Nakrem, 1995	?
		Permian	Germany	reconstructed	Ernst, 2001	?
R. tenax	24	Mississippian	Illinois Basin	measured	Snyder, 1991	3 to 12
R. tenussima	24	Mississippian	Illinois Basin	measured	Snyder, 1991	3 to 12
Spinofenestella	(39 total)					
S. antiqua	12	Devonian	Germany	reconstructed	Ernst & Schroeder, 2007	9
S. geinitzi	12	Permian	Germany	reconstructed	Ernst, 2001	6
S. inclara	2	Devonian	Czech Republic	measured	McKinney & Kriz, 1986	1
S. minuta	12	Permian	Germany	reconstructed	Ernst, 2001	7
Wjatkella	(12 total)					
W. permiana	12	Permian	Nevada	reconstructed	McColloch et al., 1994	?

*See Discussion, "Genera Represented by Single Species" for explanation of generic reassignment.